Ketohexokinase-C regulates global protein acetylation to decrease carnitine palmitoyltransferase 1a-mediated fatty acid oxidation

Robert N. Helsley, Se-Hyung Park, Hemendra J. Vekaria, Patrick G. Sullivan, Lindsey R. Conroy, Ramon C. Sun, María del Mar Romero, Laura Herrero, Joanna Bons, Christina D. King, Jacob Rose, Jesse G. Meyer, Birgit Schilling, C. Ronald Kahn, Samir Softic

Table of contents

Supplementary materials and methods

Quantification of Hepatic Lipids

Extraction of liver lipids and subsequent quantification of hepatic triglycerides and total cholesterol were conducted using enzymatic assays as previously described [1, 2]. In short, liver samples and cultured AML12 hepatocytes were delipidated in 4 mL of 2:1 chloroform to methanol (v/v) overnight. The organic solvent was dried under a constant stream of N_2 prior to adding 6 mL of 2:1 chloroform to methanol and 1.2 mL of 0.05% H_2SO_4. The samples were vortexed, spun down at 2000 rpm for 15 minutes to separate the phases. The bottom (organic) phase was recorded, and 0.5 mL of the organic phase was added to 1 mL of 1% TritonX-100 in chloroform. The samples were dried under N_2 and 0.5 mL H_2O was added prior to quantification of triglycerides and total cholesterol, per manufacturer's instructions. All standards and blanks were prepared in a similar fashion, and data were presented normalized to initial liver weights or protein concentration for AML12 hepatocytes.

Seahorse XF96 Metabolic Measurements

FFA oxidation and glycolytic and rates were measured using the SeaHorse Bioscience XF96 Cellular Flux Analyzer (Agilent Technologies), as described previously [3]. AML12 hepatocytes were seeding at 20,000 cells/well in complete DMEM media. After 24-hours, the cell media was changed to serum starvation media supplemented with 1 mM sodium pyruvate and 2mM Glutamax for 18-24 hours. The media was changed to Krebs-Henseleit Buffer and oxygen consumption rate was measured following exposure to a 0.4 mM FFA mixture (2:1 oleate to palmitate in BSA) and etomoxir [3]. For extracellular acidification rates, hepatocytes were cultured in low glucose DMEM media prior to exposure to standard glycolytic perturbations of glucose, oligomycin, and 2-deoxyglucose.

KHK Overexpression in Cultured Hepatocytes

Mouse AML12 hepatocytes were engineered to overexpress KHK-C as previously shown [4]. AML12 hepatocytes were transduced with a lentivirus containing the mouse KHK-C gene fused to GFP (Origene) at a multiplicity of infection of 5. Five days after transduction, GFP(+) cells were sorted and plated as a

single cell in a 96-well plate. Single cells were cultured in complete DMEM and subcultured in larger wells until RNA and protein analysis to confirm overexpression. Cells with the same passage number which did not exhibit KHK-C overexpression were used as controls. To confirm changes in KHK-C activity, activity assays were carried out using our previously published protocol [4].

FFA-Induced Triglyceride Accumulation in Cultured Hepatocytes

Mouse AML12 hepatocytes were cultured in DMEM/F12 (10-090-CV) containing 10% fetal bovine serum (FBS; 45000-734), 1X penicillin-streptomycin (15140122), 1X Insulin-transferrin-sodium selenite (I1884), and 40 ng/mL dexamethasone (D1756). The cells were then treated with media containing BSA (0.16% final concentration) or 0.16% BSA conjugated to 0.4 mM FFA (2:1 oleate to palmitate) [3]. After 24 hours, the hepatocytes were washed in 1X PBS and triglycerides were extracted and quantified.

Transmission Electron Microscopy

Electron microscopy was completed using a previously described protocol [3]. In short, a small piece of liver tissue (1 x 2 mm) was fixed in 2.5% paraformaldehyde, 5% glutaraldehyde, 0.06% picric acid in 0.2 M Cacodylate buffer. The samples were processed and images were captured by the Harvard Medical School Electron Microscopy Facility. Mitochondrial size was quantified from 5000x images using Image J software.

CRISPR-Cas9 Nickase Targeted Knockdown of CPT1α

The guides used to knockdown *CPT1α* were designed using the ATUM gRNA design tool, and were predicted to have the least off-target activity. For complete guide sequences, see **Sup. Table 4**. The pSpCas9n(BB)-2A-Puro (PX462) V2.0 was a gift from Feng Zhang (Addgene plasmid #62987; http://n2t.net/addgene:62987; RRID:Addgene_62987) [5]. The PX462 plasmid was used as a backbone to clone in guide sequences targeting *CPT1α*, using a previously published protocol from the Zhang Lab [5]. In brief, 1 µg of plasmid was first digested using FastDigest *BbsI* and FastAP in 10X FastDigest Buffer (Fisher), and gel purified using the QIAquick Gel Extraction kit. The primers were then phosphorylated using T4 PNK in 10X T4 Ligation Buffer and annealed. The guides were ligated into the plasmid using 1X Quick Ligase (NEB M2200), and underwent transformation in ultracompetent DH5α cells (18-265-017; Invitrogen). All plasmid DNA was isolated using QIAprep Spin Miniprep kit (Qiagen 27104) and

sequenced accordingly.

Mouse AML12 hepatocytes were cultured in DMEM/F12 (10-090-CV) containing 10% fetal bovine serum (FBS; 45000-734), 1X penicillin-streptomycin (15140122), 1X Insulin-transferrin-sodium selenite (I1884), and 40 ng/mL dexamethasone (D1756). Cells were transfected using Fugene 6 (3:1 ratio) in 24-well plates (VWR 82050-892) with 0.75 µg of PX462 containing no guides (control) or PX462 containing guides targeting *CPT1α*. Twenty-four hours post-transfection, cells were treated with 0.75 µg/mL of puromycin for 5 consecutive days. This dose of puromycin was selected based off a dose-response curve to identify the lowest concentration to kill 100% of the cells (data not shown). After 5-days, media was changed to complete media without puromycin. Clones were scraped into separate wells in a 96-well plate, grown to confluency, and then subcultured to larger 6-well plates for protein isolation and western blot.

Acetyl-CoA Quantification

Acetyl-CoA levels were measured in WT and KHK-C OE AML12 hepatocytes using the PicoProbe™Acetyl-CoA Fluorometric Assay Kit (BioVision) according to manufacturers instructions. In short, five 10 cm plates of both WT and OE hepatocytes were washed in ice-cold 1X PBS prior to lysing the cells with lysis buffer containing 1X protease and phosphatase inhibitor cocktail (bimake.com). 1.5 mg of cellular protein was deproteinized with 3 µl of 1 N perchloric acid then neutralized with 3 M KOH (1 µl/10 µl of cellular lysate). The lysate was centrifuged at 10,000 x g, and 10 µl of supernatant was diluted with 40 ul of assay buffer for the fluorometric assay. All samples were completed in duplicate and one additional sample omitting the conversion enzyme was used to subtract out background for each sample. After a 10 minute incubation with the CoA conversion mixture, fluorescence was measured using excitation/emission of 535/587 nm in a black 96-well plate. Five µl of cellular lysate was allocated for protein concentration measurements via the Pierce™ Bicinchoninic Acid Protein (BCA) assay (ThermoFisher). Data were reported by normalizing the concentration of acetyl-coA to total protein levels.

Real-Time PCR Analysis of Gene Expression

Tissue RNA extraction, cDNA synthesis and quantitative real-time PCR was performed as previously described [3, 6]. A small portion of frozen livers (~20 mg) was homogenized in 1 mL of QIAzol (Qiagen

79306). After the addition of 200 µL of chloroform, phase separation occurred by centrifugation. The top layer was mixed with 400 µL of 75% ethanol prior to running the sample over a RNeasy spin column (Qiagen, RNeasy Mini Kit). 500 ng of RNA was used as a template to synthesize cDNA (High Capacity cDNA Reverse Transcription Kit, Applied Biosystems). QPCR reactions were carried out using 2X SYBR green (Cowin Biosciences) and mRNA expression levels were calculated based off a standard curve using the Applied Biosystems (ABI) QuantStudio 7 Flex Real-Time PCR System. Primers used for qPCR are listed in **Sup. Table 3**.

SDS-PAGE Immunoblotting

Tissue and cellular protein extracts were solubilized in 1 mL of lysis buffer containing 25 mM Tris-HCl (pH=7.4), 100 mM NaF, 50 mM $Na_4P_2O_7$, 10 mM EGTA, 10 mM EDTA, and 1% NP-40, as previously indicated [3]. The lysis buffer was supplemented with 1X protease and phosphatase inhibitor cocktail (bimake.com). Protein was isolated and quantified via the Pierce™ Bicinchoninic Acid Protein (BCA) assay (ThermoFisher). For SDS-PAGE, 10 µg of protein was loaded and separated on 4-15% criterion TGX gels. Proteins were blocked with 5% milk and probed with antibodies listed in the Key Resources Table.

Mitochondria Substrate Assay

Mitochondria substrate metabolism was assayed using mitochondria substrate plates (MitoPlate S-1) from BioLog [7]. In brief, 30 ul of the assay mix, containing Biology MAS, Redox Dye, and Saponin (to induce cell permeability), were added to the 96 well plate to incubate at 37˚C for 1 hour. WT and KHK-C OE AML12 hepatocytes were then harvested and suspended in 1X Biolog MAS buffer, filtered through a 70 µm filter (Falcon 352350), and counted. A total of 28,500 cells were then added to each well. The color formation was read kinetically using OD590. Data was normalized to control wells containing no substrate (i.e. background), and were expressed as a rate of substrate utilized. All substrates were completely utilized in the first 45 minutes of the assay.

Metabolomics

Metabolomics analysis was completed using a similar protocol as previously described [3]. In brief, 50 mg of liver tissue was homogenized in 1 mL of 50% aqueous acetonitrile containing 0.3% formic acid.

Liver amino acids, acyl-CoAs and organic acids, and acylcarnitines were analyzed using stable isotope dilution techniques by GC/MS and MS/MS as shown prior.

Proteomics Analysis

Protein digestion and desalting

Cell pellets of wild type and KHK-C OE AML-12 hepatocytes, with 4 replicates each, were solubilized in 700 µL of lysis buffer containing 8 M urea, 200 mM triethylammonium bicarbonate (TEAB), pH 8, 75 mM sodium chloride, 1 µM trichostatin A, 3 mM nicotinamide, and 1x protease/phosphatase inhibitor cocktail (Thermo Fisher Scientific, Waltham, MA), and sonicated using a probe sonicator. Protein concentrations were determined using a BCA Assay (Thermo Fisher Scientific, Waltham, MA). Proteins (2.1 mg) were reduced using 20 mM dithiothreitol (DTT) in 50 mM TEAB for 30 min at 37 °C, and after cooling to room temperature, alkylated with 40 mM iodoacetamide (IAA) for 30 min at room temperature in the dark. Samples were diluted 4-fold with 50 mM TEAB, pH 8, and proteins were digested overnight with a solution of sequencing-grade trypsin (Promega, San Luis Obispo, CA) in 50 mM TEAB at a 1:50 (wt:wt) enzyme:protein ratio at 37°C. This reaction was quenched with 1% formic acid (FA) and the sample was clarified by centrifugation at 2,000 x g for 10 min at room temperature. Clarified peptide samples were desalted with Oasis 10-mg Sorbent Cartridges (Waters, Milford, MA). 100 µg of each peptide elution were aliquoted for analysis of protein-level changes, after which all desalted samples were vacuum dried. The 100 µg whole lysate aliquots were re-suspended in 0.2% FA in water at a final concentration of 1 µg/µL. The remaining 2 mg digests were re-suspended in 1.4 mL of immunoaffinity purification (IAP) buffer (Cell Signaling Technology, Danvers, MA) containing 50 mM 4-morpholinepropanesulfonic acid (MOPS)/sodium hydroxide, pH 7.2, 10 mM disodium phosphate, and 50 mM sodium chloride for PTM enrichment. Peptides were enriched for acetylation with anti-acetyl antibody conjugated to agarose beads from the Acetyl-Lysine Motif Kit (Cell Signaling Technology, Danvers, MA). This process was performed according to the manufacturer's protocol, however each sample was incubated in a quarter of the recommended volume of washed beads. Peptides were eluted from the antibody-bead conjugates with 0.15% trifluoroacetic acid in water and were desalted using C18 stage tips made in-house. Samples were vacuum dried and re-suspended in 20 µL of 0.2% FA in water. Finally, indexed retention time standard

peptides (iRT; Biognosys, Schlieren, Switzerland) [8] were spiked in the samples according to manufacturer's instructions.

Mass Spectrometric Analysis

LC-MS/MS analyses were performed on a Dionex UltiMate 3000 system online coupled to an Orbitrap Eclipse Tribrid mass spectrometer (Thermo Fisher Scientific, San Jose, CA). The solvent system consisted of 2% ACN, 0.1% FA in water (solvent A) and 98% ACN, 0.1% FA in water (solvent B). Briefly, proteolytic peptides were loaded onto an Acclaim PepMap 100 C18 trap column with a size of 0.1 x 20 mm and 5 µm particle size (Thermo Fisher Scientific) for 5 min at 5 µL/min with 100% solvent A. For the protein lysates, 400 ng was loaded (protein level analysis), and for the enriched acetylated peptides (PTM level analysis), 4 µL of each PTM-enriched sample was injected. Peptides were eluted on to an Acclaim PepMap 100 C18 analytical column sized as follows: 75 µm x 50 cm, 3 µm particle size (Thermo Fisher Scientific) at 0.3 µL/min using the following gradient of solvent B: 2% for 5 min, linear from 2% to 20% in 125 min, linear from 20% to 32% in 40 min, and up to 80% in 1 min, with a total gradient length of 210 min. All samples were acquired in data-independent acquisition (DIA) mode [9, 10]. Full MS spectra were collected at 120,000 resolution (AGC target: 3e6 ions, maximum injection time: 60 ms, 350-1,650 m/z), and MS2 spectra at 30,000 resolution (AGC target: 3e6 ions, maximum injection time: Auto, NCE: 27, fixed first mass 200 m/z). The DIA precursor ion isolation scheme consisted of 26 variable windows covering the 350-1,650 m/z mass range with an overlap of 1 m/z (**Sup. Table 5**) [11].

Data Analysis

DIA Data Processing and Statistical Analysis

DIA data was processed in Spectronaut (version 15.1.210713.50606) using directDIA for both the protein level as well as PTM-enriched samples. Data was searched against a database containing all Mus musculus entries extracted from SwissProt (17,090 protein entries; January 27, 2022). Trypsin/P was set as digestion enzyme and two missed cleavages were allowed. Cysteine carbamidomethylation was set as fixed modification, and methionine oxidation and protein N-terminus acetylation as variable

modifications. Data extraction parameters were set as dynamic. Identification was performed requiring a 1% q-value cutoff on the precursor ion and protein level. For the protein lysate samples, quantification was based on the peak areas of extracted ion chromatograms (XICs) of 3 – 6 MS2 fragment ions, and local normalization was applied. iRT profiling was selected. For the PTM-enriched samples, lysine acetylation was additionally set as variable modification. PTM localization was selected with a probability cutoff of 0.75. Quantification was based on the peak areas of XICs of 3 – 6 MS2 fragment ions, without normalization as well as data filtering using q-value sparse. Grouping and quantitation of PTM peptides were accomplished using the following criteria: minor grouping by modified sequence and minor group quantity by mean precursor quantity.

Differential expression analysis comparing KHK-C OE to wild-type mouse hepatocytes was performed using a paired t-test, and p-values were corrected for multiple testing, specifically applying group wise testing corrections using the Storey method [12]. For whole lysate (protein level) analysis, protein groups are required to have at least two unique peptides. For determining differential protein changes, a q-value < 0.01 and absolute Log2(fold-change) > 0.58 are required to qualify as 'significantly-altered' (**Sup. Table 2**). For the PTM analysis, each acetylated peptide is quantified individually comparing conditions with significance cutoffs of p-value < 0.05, and absolute Log2(normalized fold-change) > 0.58 (**Sup. Table 1**).

Clustering Analysis

Partial least squares-discriminant analysis (PLS-DA) of the proteomics data was performed using the package mixOmics [13] in R (version 4.0.2; RStudio, version 1.3.1093).

Pathway Enrichment Analysis

Over-representation analyses (ORA) were performed using Consensus Path DB-mouse (Release MM11, 14.10.2021) [14, 15] to evaluate which gene ontology terms were significantly enriched. Gene ontology terms identified from the ORA were subjected to the following filters: q-value < 0.05, term category = b (biological process), and term level > 3. Dot plots were generated using the ggplot2 package [16] in R (version 4.0.5; RStudio, version 1.4.1106) to visualize significantly-enriched biological processes.

Data and code availability

Raw data and complete MS data sets have been uploaded to the Center for Computational Mass Spectrometry, to the MassIVE repository at UCSD, and can be downloaded using the following link: https://massive.ucsd.edu/ProteoSAFe/dataset.jsp?task=b9ba416b2a0b44c8b34a29e3228e6eb3 (MassIVE ID number: MSV000089882; ProteomeXchange ID: PXD035316).

[Note: To access the data repository MassIVE (UCSD) for MS data, please use: Username: MSV000089882_reviewer; Password: winter].

Statistical Analysis

The generation of graphs and statistical analyses were completed using GraphPad Prism 9.3.0. Data are expressed as ±SEM, unless otherwise noted in the figure legend. Statistical tests used for each panel of data can be found within the figure legend. Differences were computed using a combination of two- and one-way ANOVAs followed by Sidak and Dunnett's *post hoc* analysis, respectively. When comparing two groups, a Student's t-test was used. P-values <0.05 were considered statistically significant.

Supplementary figure legends

Fig. S1. Short-Term Sugar Supplementation Does Not Alter Body Weight and Insulin Sensitivity. (**A**) An overview of the experimental design. (**B**) Final body weights from the mice across all six groups. (**C**) Total calories from water (red) and pellet food (blue) over the course of the 2-week experiment presented as kcal/mouse/day. (**D, E**) Oral glucose tolerance test performed after 7 days on the diet **(D)** and area under the curve was quantified (**E**, n=8). (**F**) Fasting insulin levels were measured after 7 days on diet (n=5-6). (**G**) To assess hepatic insulin sensitivity, mice were injected with saline or 1 IU insulin into the inferior vena cava 10 minutes prior to tissue collection. Western blot analysis of phosphorylation of the insulin receptor β (IRβ) at tyrosine 1150, total IRβ, phosphorylation of Akt serine/threonine kinase (Akt) at serine 473, total Akt, phosphorylation of extracellular signal-regulated kinase (Erk) at threonine 202/tyrosine 204, and total Erk from liver tissue of saline and insulin injected animals. Significance was determined using repeated measures ANOVA for the oral glucose tolerance tests in panel D with *P*-values provided. For all other panels, significance was determined by two-way ANOVA with Sidak's *post hoc* analysis comparing sugar-supplemented groups to their respective chow and HFD controls. Chow versus HFD control comparisons were completed using a *post hoc* Student's *t*-test. Significance is denoted using ($) comparing sugar supplemented groups to their chow+H_2O control, (*) comparing HFD+H_2O to chow+H_2O group, or (#) denotes significance of sugar supplemented groups compared to their HFD+H_2O control. $^{*,\#}P<0.05$; $^{****,\#\#\#\#}P<0.0001$.

Fig. S2. Sugar Supplementation for Two weeks Does Not Activate Lipogenic Transcription Factors. (**A**) The essential fatty acyl-CoAs, linoleoyl and linolenoyl, were quantified by mass spectrometry (n=6). (**B**) Nuclear ChREBP and SREBP1 protein levels were measured using western blot. Lamin A/C serves as the loading control. (**C**) Nuclear ChREBP and SREBP1 protein levels were quantified by densitometry from panel B (n=4). (**D**) QPCR quantification of mRNA expression for *Chrebpβ*, and *Acss2* (n=7-8). All QPCR data are normalized to the average of the housekeeping genes, 18S and TBP. Densitometry quantification of western blot data in Fig 1F for ACSS2 (n=4). (**E**) Western

blot for ACLY measured at basal level (BL) and after treatment with Cyclohexamide (CHX) or CHX plus fructose (C+Fru) in wild type (WT) and KHK-C OE cells. Significance was determined by two-way ANOVA with Sidak's *post hoc* analysis comparing sugar-supplemented groups to their respective chow and HFD controls. Chow versus HFD control comparisons were completed using a *post hoc* Student's *t*-test. Significance is denoted using ($) comparing sugar supplemented groups to their chow+H_2O control, (*) comparing HFD+H_2O to chow+H_2O group, or (#) denotes significance of sugar supplemented groups compared to their HFD+H_2O control. $^{**,\#\#}P<0.01$; $^{***,\#\#\#}P<0.001$; $^{****,\#\#\#\#}P<0.0001$.

Fig. S3. Sugar Supplementation Minimally Affects TCA Cycle and Amin Acid Metabolism in the Liver. (**A**) Mass spectrometry quantification of TCA cycle intermediates in the liver (n=6). Hepatic levels of tyrosine (**B**) and amino acids involved in urea cycle (**C**) and non-essential amino acids (**D**) as measured by mass spectrometry (n=6). Significance was determined by two-way ANOVA with Sidak's *post hoc* analysis comparing sugar-supplemented groups to their respective chow and HFD controls. Chow versus HFD control comparisons were completed using a *post hoc* Student's *t*-test. Significance is denoted using ($) comparing sugar supplemented groups to their chow+H_2O control, (*) comparing HFD+H_2O to chow+H_2O group, or (#) denotes significance of sugar supplemented groups compared to their HFD+H_2O control. $^{*,\#}P<0.05$; $^{**,\#\#}P<0.01$; $^{***,\#\#\#}P<0.001$.

Fig. S4. Glucose Supplementation of HFD Increases Fructolysis Gene Expression. (**A, B**) mRNA levels of *Khkc, Aldob*, *Tkfc*, *Ar,* and *Sdh* were measured by QPCR (n=7-8). All QPCR data are normalized to the average of the housekeeping genes, 18S and TBP. (**C**) A graphical representation of the carnitine shuttle pathway. (**D, E**) Hepatic protein levels of the FAO proteins OCTN2, CACT, CPT2, ACADVL, and ACADL assessed by western blot (**D**) and quantified by densitometry (**E**) across the six groups (n=4). Ponceau stain was used as a loading control. Significance was determined by two-way ANOVA with Sidak's *post hoc* analysis comparing sugar-supplemented groups to their respective chow and HFD controls. Chow versus HFD control comparisons were completed using a *post hoc* Student's *t*-test.

Significance is denoted using ($) comparing sugar supplemented groups to their chow+H_2O control, (*) comparing HFD+H_2O to chow+H_2O group, or (#) denotes significance of sugar supplemented groups compared to their HFD+H_2O control. **,##P<0.01; ***,###P<0.001; ****,####P<0.0001.

Fig. S5. KHK-C Inversely Associates with CPT1a Protein Levels in Mice with Metabolic Dysfunction. (**A**) QPCR was used to measure mRNA levels of *Octn2, Cact, Crat, Acadvl, Acadl, Acadm,* and *Acads* (n=7-8). All QPCR data are normalized to the average of the housekeeping genes, 18S and TBP. Significance was determined by two-way ANOVA with Sidak's *post hoc* analysis comparing sugar-supplemented groups to their respective chow and HFD controls. Chow versus HFD control comparisons were completed using a *post hoc* Student's *t*-test. Significance is denoted using ($) comparing sugar supplemented groups to their chow+H_2O control, (*) comparing HFD+H_2O to chow+H_2O group, or (#) denotes significance of sugar supplemented groups compared to their HFD+H_2O control. **(B-E)** KHK-C, CPT1a, and Vinculin protein levels were measured by western blot in HFD-fed mice receiving KHK AAV or KHK siRNA (**B;** n=4), in FIRKO mice receiving control or KHK siRNA (**C;** n=4), in WT and db/db mice (**D;** n=4), and in WT mice fed chow treated with control or KHK-C AAV (**E;** n=3). Significance was determined by one way ANOVA using a *post hoc* Dunnett's test (**B**, **C**) or a Student's t-test (**D**). All western blot quantification is provided. *,#P<0.05; **,##P<0.01; ***,###P<0.001, **** P<0.0001

Fig. S6. Selective KHK-C OE in AML12 Hepatocytes. (**A**) Protein levels of ALDOB, TKFC, AR, SDH, and Vinculin (VINC) loading control were measured in WT, KHK-C OE AML12 hepatocytes, and WT liver (L) as a control. (**B**) KHK activity was measured from WT and KHK-C OE AML12 hepatocytes treated with fructose (n=4). (**C, D**) Hepatic protein levels of the FAO proteins ACADVL, ACADL, ACADS assessed by western blot (**C**) and quantified by densitometry (**D**) (n=3). (**E**) Seahorse FAO assay recording oxygen consumption rate (OCR) in WT and KHK-C OE AML12 hepatocytes at baseline (n=10-11). Significance was determined by a Student's two-tailed *t*-test. Significance is defined as ****P<0.0001.

Fig. S7. KHK-C Overexpression Promotes the Oxidation of Pyruvate and Citrate. (**A**) The rate of

substrate utilization for several metabolites using the MitoPlates assay with WT and KHK-C OE hepatocytes (n=5). (**B-D**) The fold change and rate of oxidation for pyruvate (**B**), citrate (**C**), and serine (**D**) between WT and OE hepatocytes (n=5). (**E**) Hepatic serine and glycine levels measured by mass spectrometry across all water and sugar supplemented groups (n=6). Significance was determined by a Student's two-tailed *t*-test for panels A-D. For panel E, significance was determined by two-way ANOVA with Sidak's *post hoc* analysis comparing sugar-supplemented groups to their respective chow and HFD controls. Chow versus HFD control comparisons were completed using a *post hoc* Student's *t*-test. Significance is denoted using ($) comparing sugar supplemented groups to their chow+H_2O control or (#) denotes significance of sugar supplemented groups compared to their HFD+H_2O control. $^{*,\#}P<0.05$; $^{**,\#\#}P<0.01$.

Fig. S8. CRISPR/Cas9N Targeting of Endogenous CPT1α in AML12 Hepatocytes. (**A**) The primers used to target exon 6 of the *CPT1α* locus. Highlighted in red are the protospacer adjacent motifs (PAM) sequences. (**B**) CPT1a protein levels were quantified by western blot from 2 WT and 5 CPT1α KD clones. Actin serves as a loading control. Clones 4 and 5 were used for subsequent analysis. (**C**) Carnitine shuttle/FAO protein levels (CPT1a, CACT, OCTN2, CPT2, ACADVL, ACADL, ACADS) were measured by western blot in WT and CPT1a knockdown clone 5 (KD-5) (**Fig. 5A**) and were further quantified by densitometry (**C**) using Actin as a loading control (n=3). (**D**) WT and CPT1α KD-4 hepatocytes were treated with 0.4 mM FFA and were stained with Nile Red (lipid droplets; red) and DAPI (nuclei; blue). 40X magnification and scale bar = 50 μm. Significance was determined using unpaired, Student's *t*-test. Significance is defined as *P<0.05; **P<0.01; ***P<0.001; ****P<0.0001.

Fig. S9. Nutrient-Induced Acetylation at CPT1α K508 is Associated with Lower CPT1α Protein. (**A-D**) Volcano plots highlighting all identified acetylation sites between the two dietary groups. Blue dots represent significantly changed acetylation sites and CPT1α acetylation sites are highlighted in red. The horizontal black bar denotes the significance cutoff of FDR = 0.01. The vertical black bars denote a minimal threshold for effect size of 1.5 (Log_2 fold change = ±0.58). Quantification of total CPT1α protein

levels (**right of volcano plot**) normalized to Vinculin (loading control) across the respective two groups. Significance was determined using unpaired, Student's two-tailed *t*-test. *P<0.05; ****P<0.0001.(**E**) QPCR quantification of mouse CPT1α mRNA in African green monkey COS-7 kidney cells transfected with plasmids encoding β-galactosidase (β-gal), WT CPT1α, and mutant K195Q, K508Q, and K634Q CPT1α. Significance was determined using one way ANOVA with **P<0.01; ***P<0.001. (**F**) Densitometry quantification for c-MYC of western blot in Fig 6F normalized to Actin loading control. Significance was determined using unpaired, Student's *t*-test. with **P<0.01.

Fig. S10. KHK-C OE Alters the Proteome in AML12 Hepatocytes and Regulates Sirtuin 2 Protein Levels In Vivo. (**A**) Pan-acetylation was measured in WT and KHK-C OE cells treated with HDAC inhibitors, Trichostatin A (TSA) and Nicotinamide (NAD). (**B**) A volcano plot highlighting proteins that are significantly different between WT and KHK-C OE AML-12 cells. Proteins in blue are increased in WT and proteins in red increased in KHK-C OE cells. The horizontal black bar denotes the significance cutoff of *Q*-value = 0.01. The vertical black bars denote a minimal threshold for effect size of 1.5 (Log_2 fold change = ±0.58). (**C, D**) Protein levels of Sirtuins (SIRTs 1, 6, 7) were measured by western blot in WT and KHK-C OE (**C**) and were quantified by densitometry (**D**) using Vinculin (VINC) as a loading control (n=3). (**E**) Sirtuin mRNA levels were measured by QPCR in WT and KHK-C OE hepatocytes (n=6). (**F-H**) SIRT1, SIRT2, CPT1a, and Vinculin protein levels were measured by western blot using liver samples from mice fed HFD, HFD+fructose, and HFD+glucose when treated with control or KHK siRNA (**F**, **G**), and was quantified by densitometry (**H**). Significance was determined using unpaired, Student's two-tailed *t*-test. **P<0.01.

Supplemental Figure 1

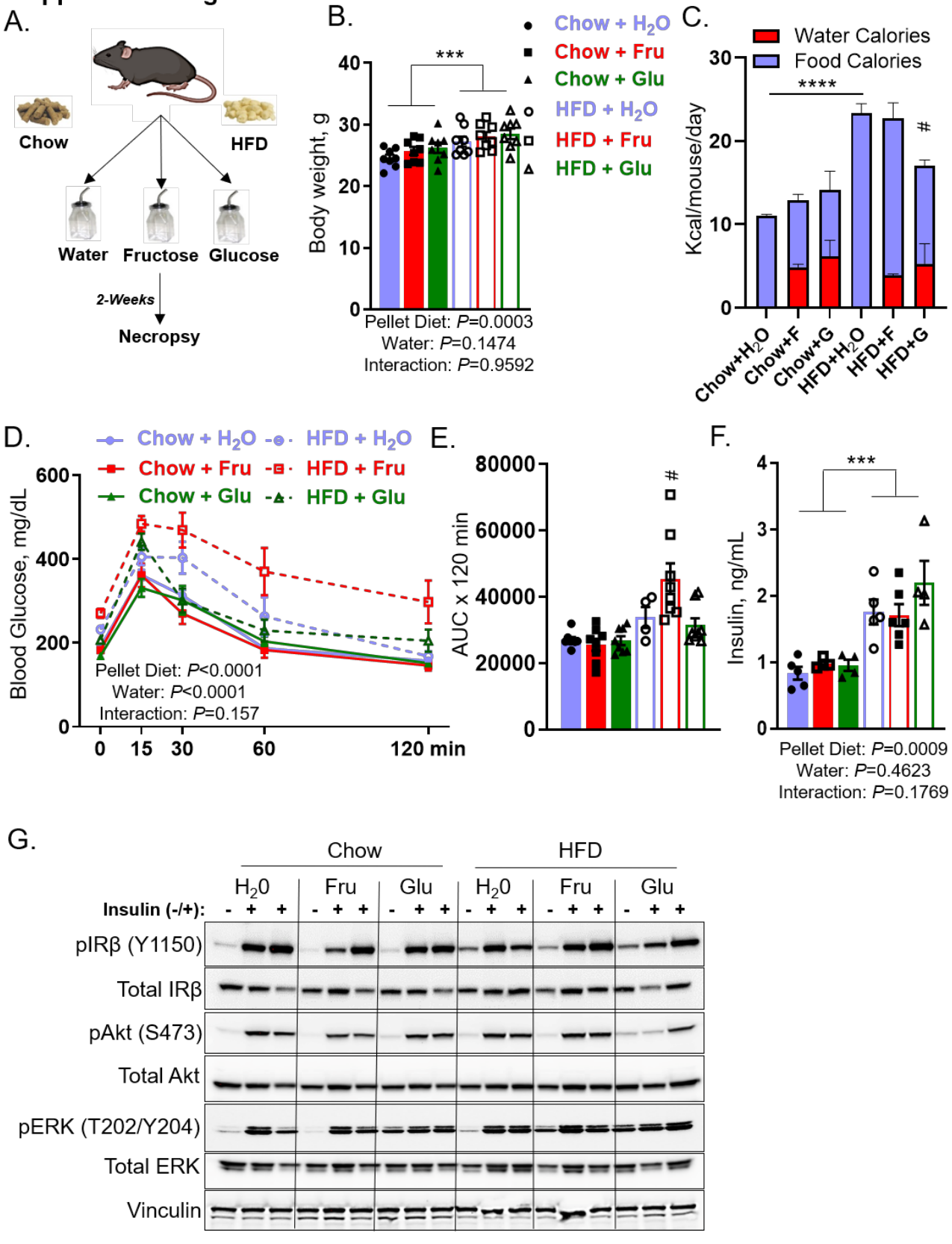

Supplemental Figure 2

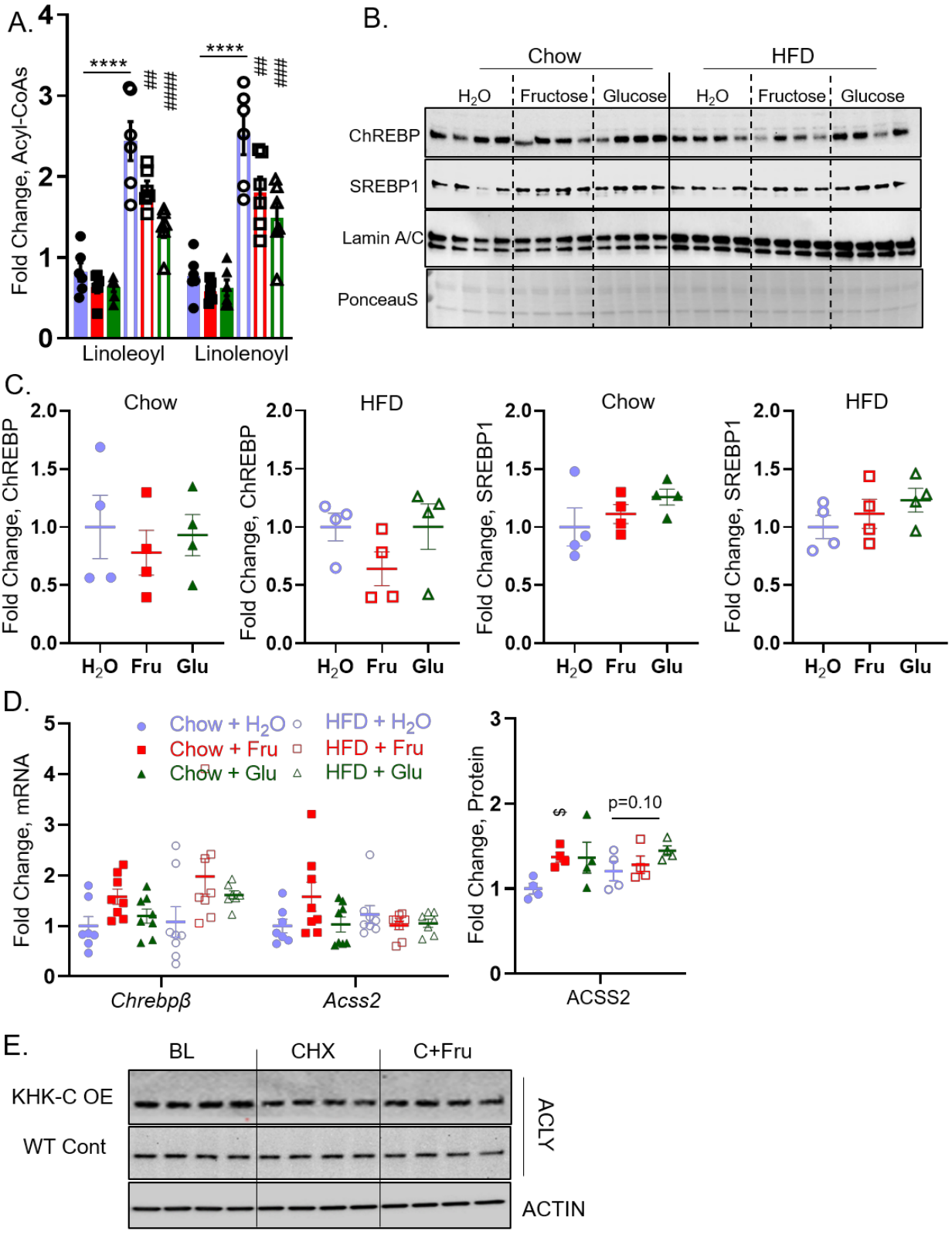

Supplemental Figure 3

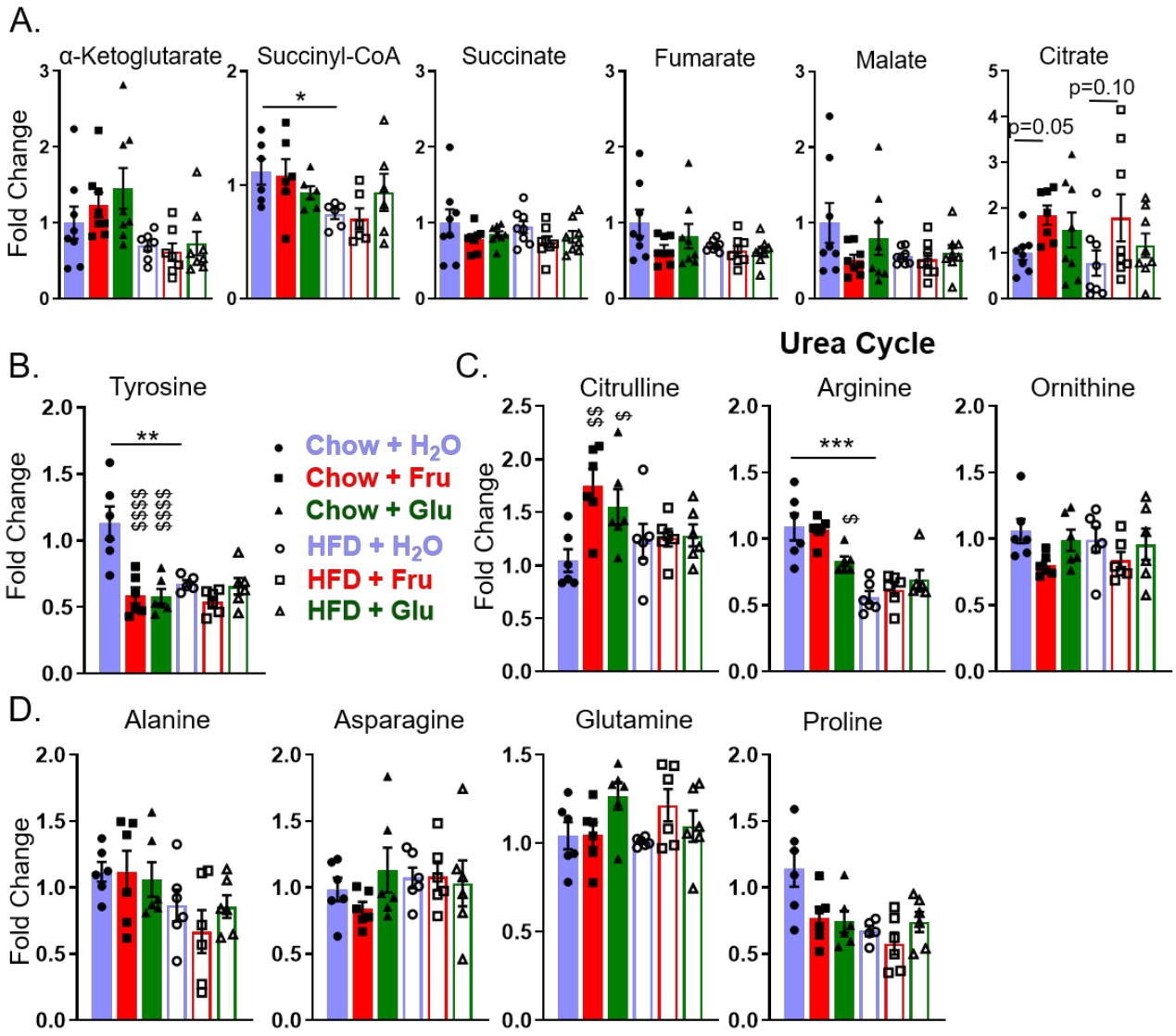

Supplemental Figure 4

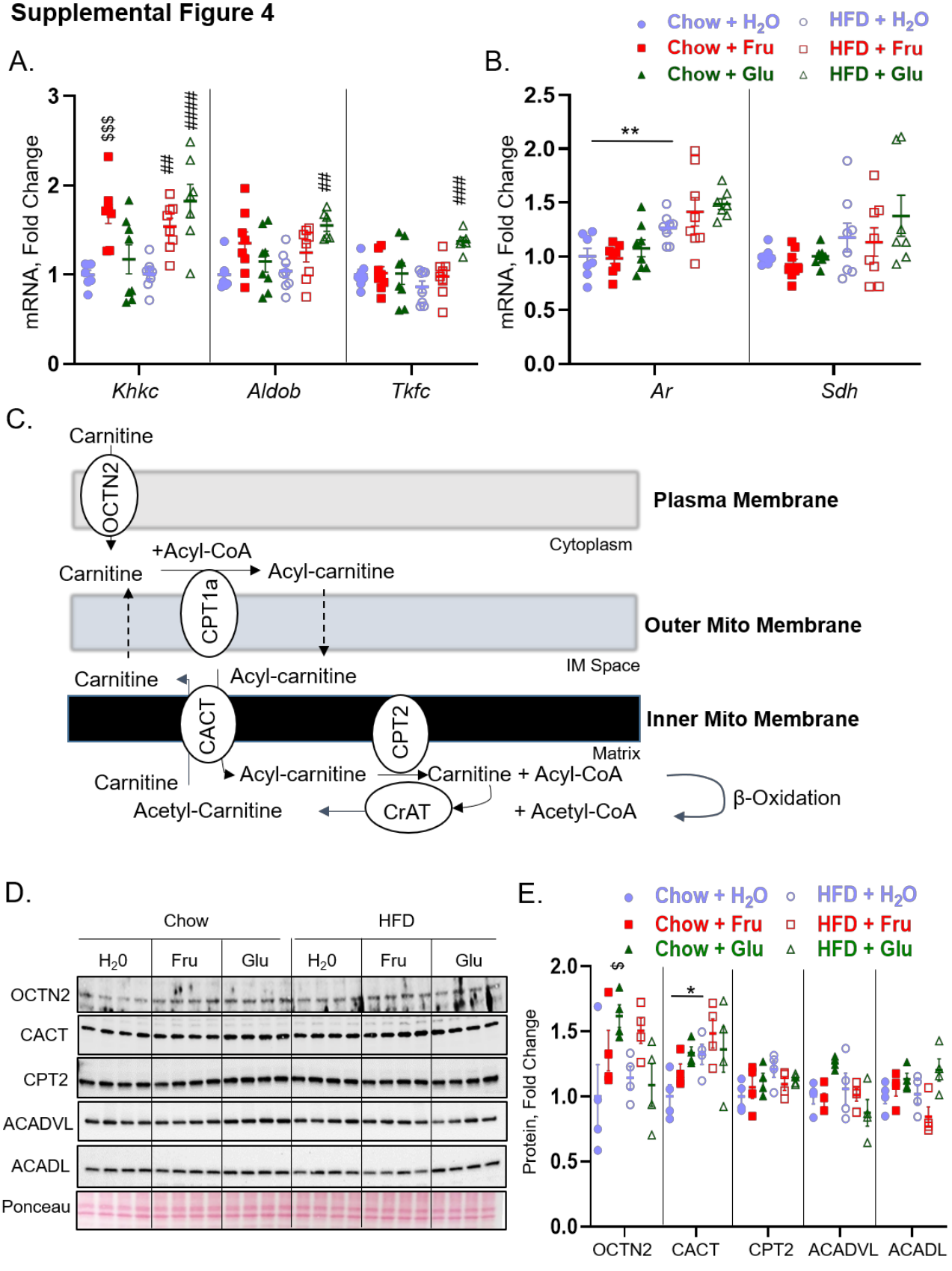

Supplemental Figure 5

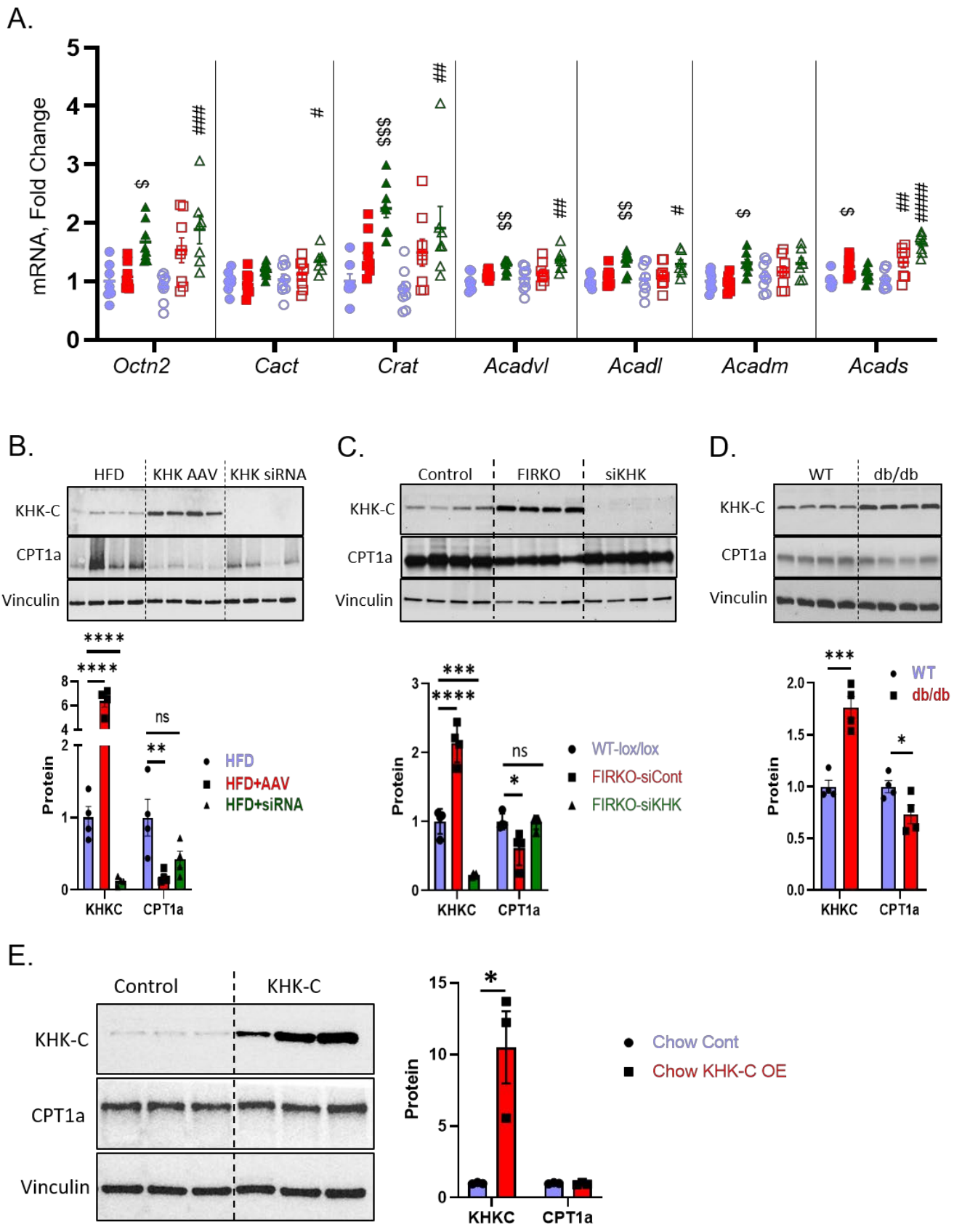

Supplemental Figure 6

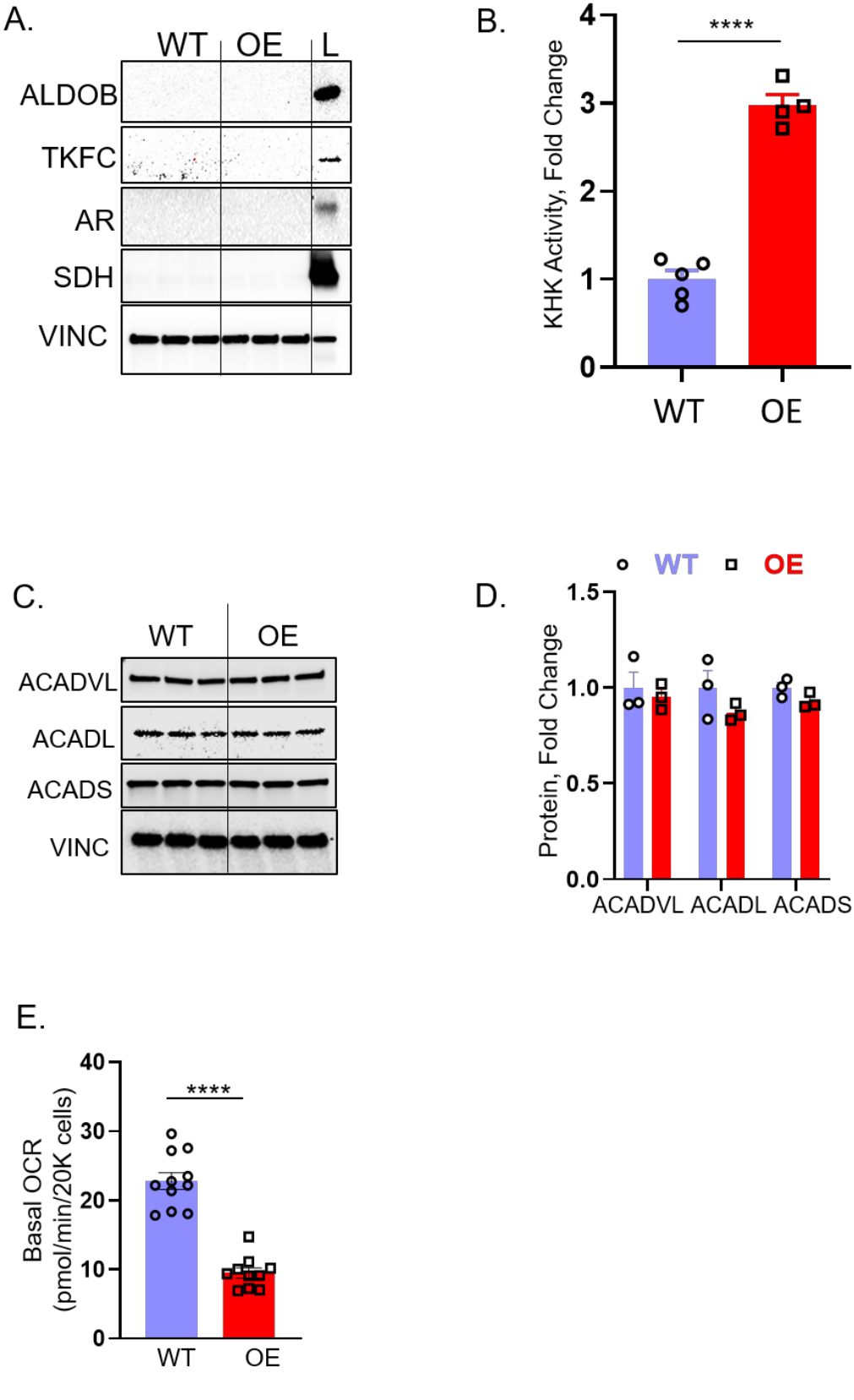

Supplemental Figure 7

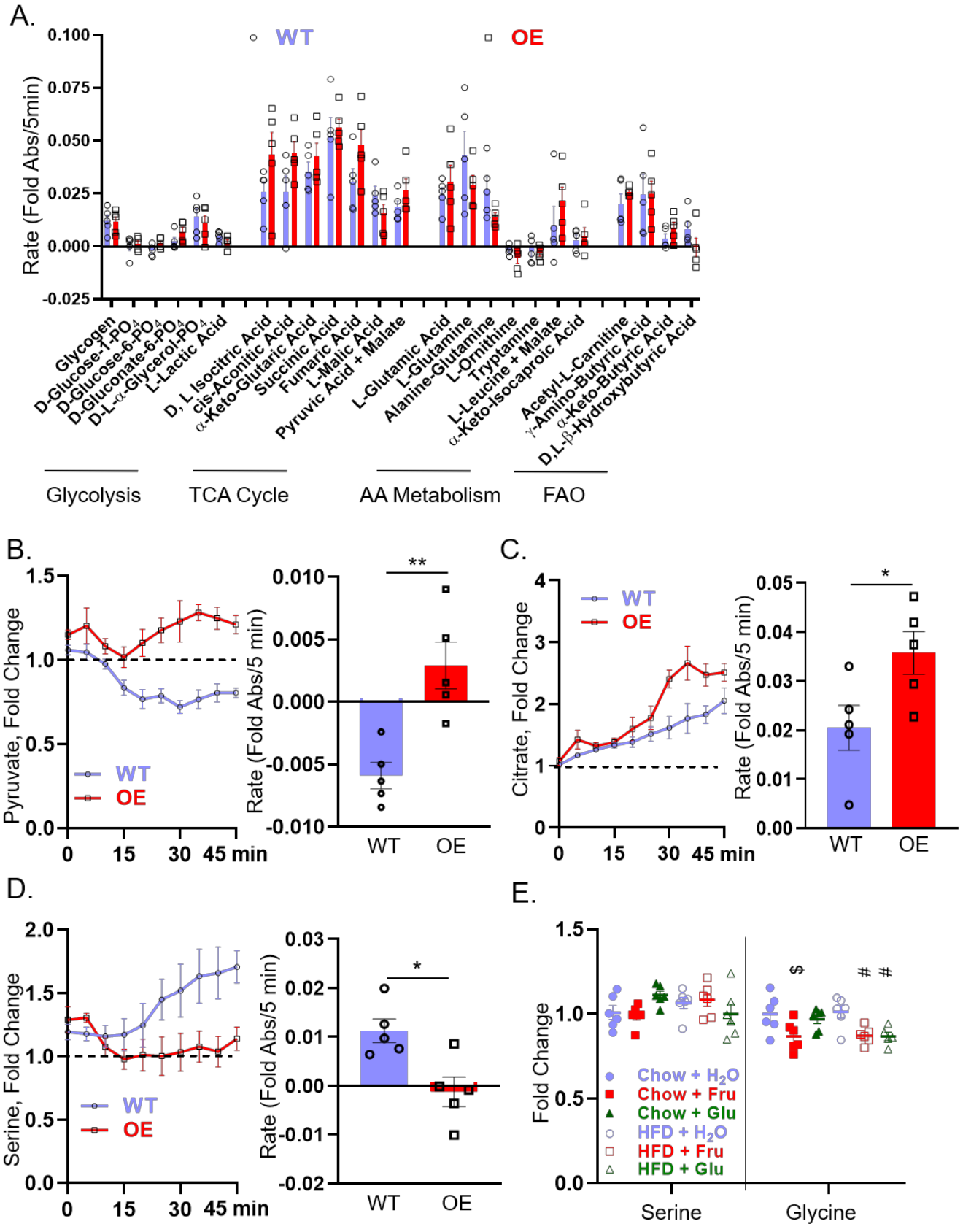

Supplemental Figure 8

A.

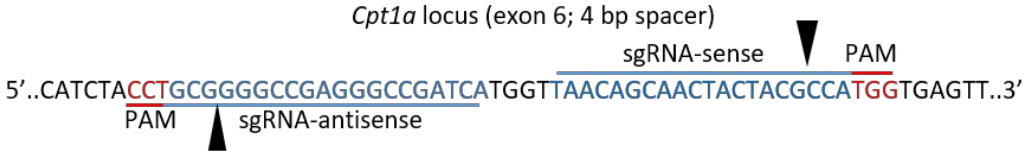

B.

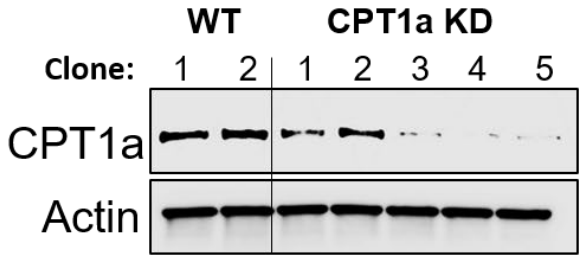

C.

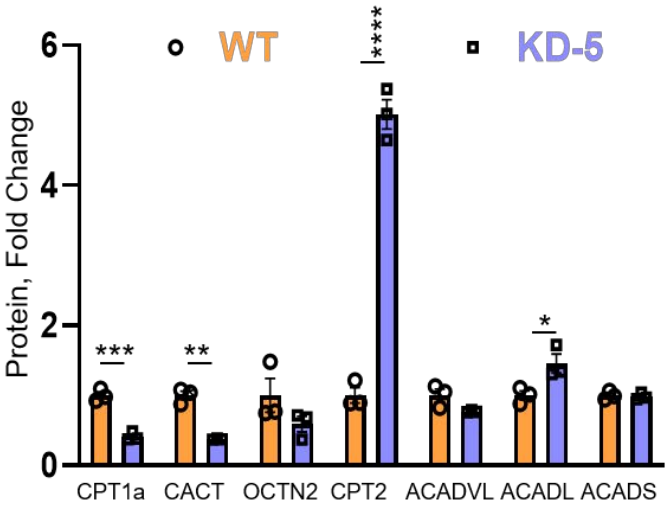

D.

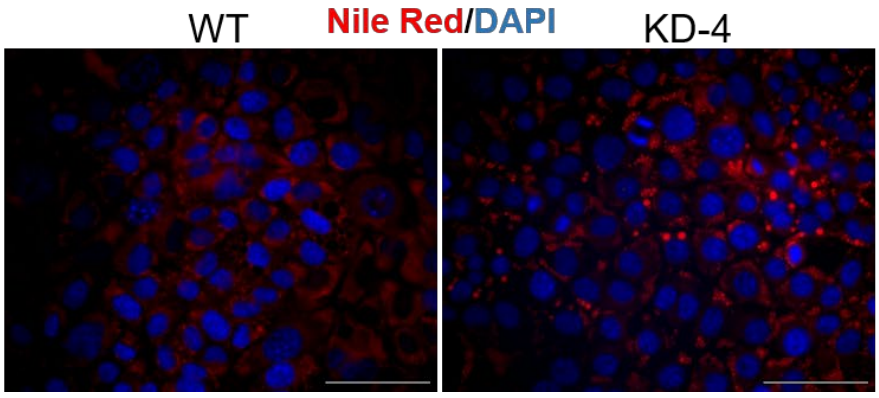

Supplemental Figure 9

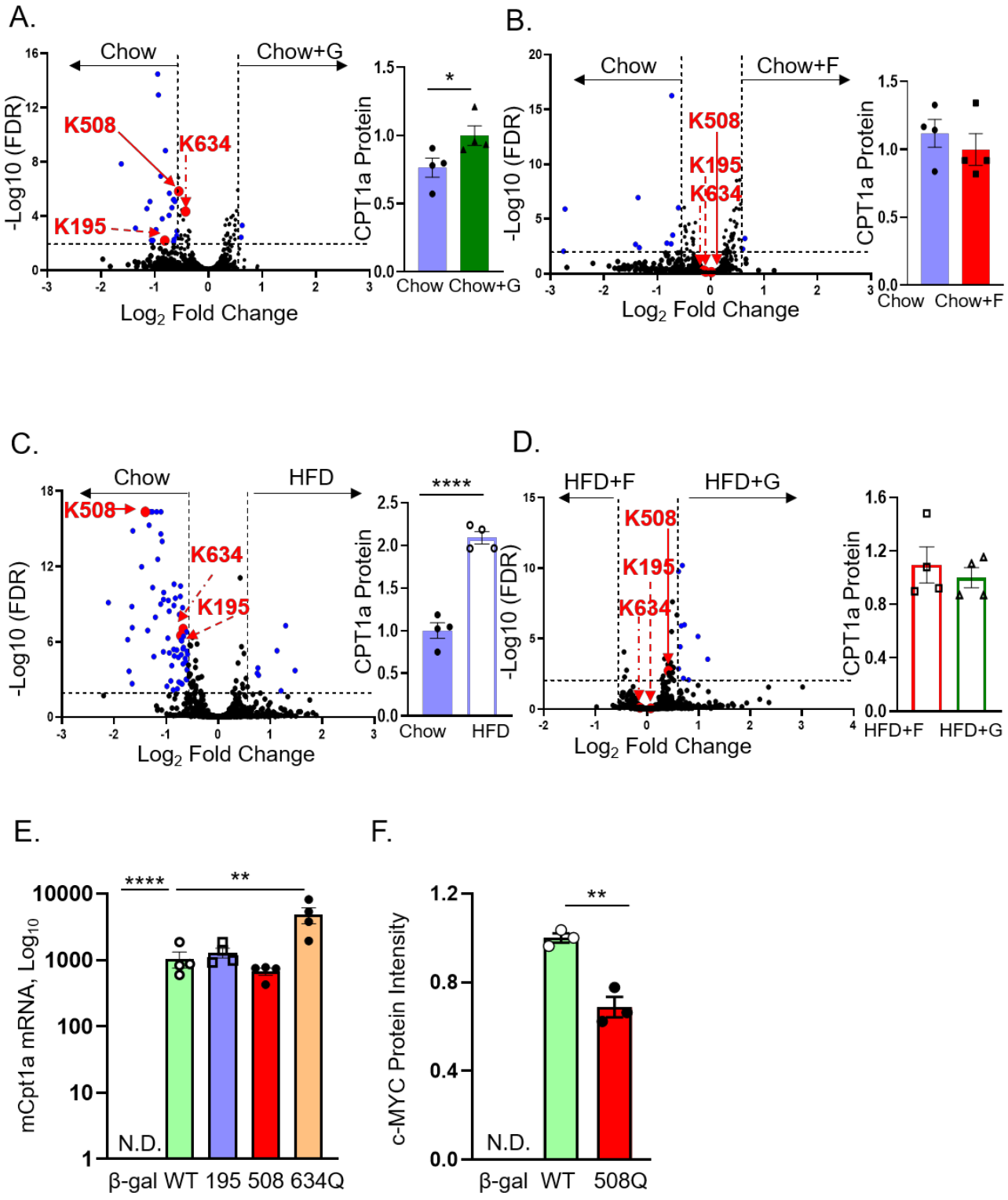

Supplementary Figure 10

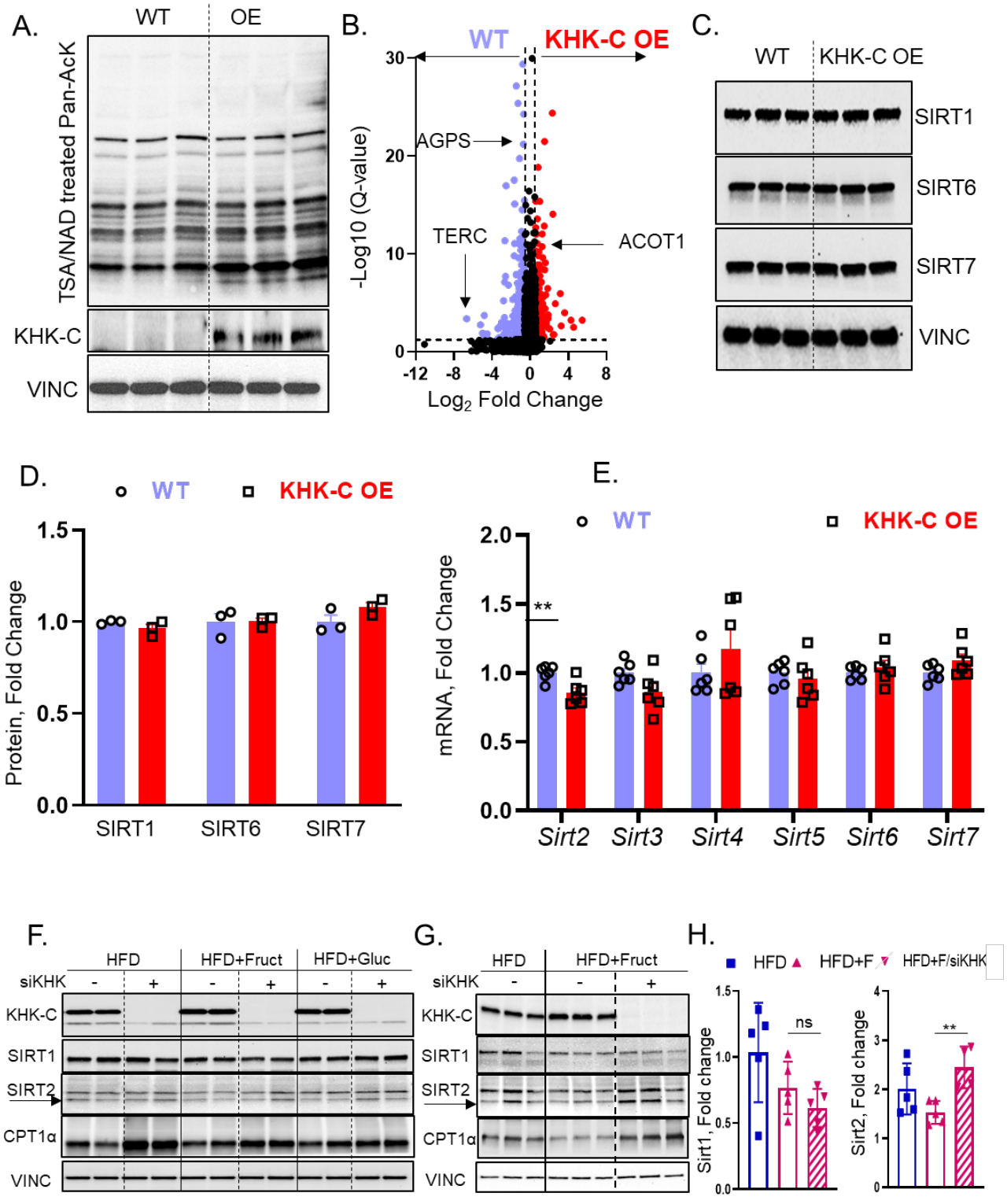

Supplemental Figure 11 – Blots from Figure 1

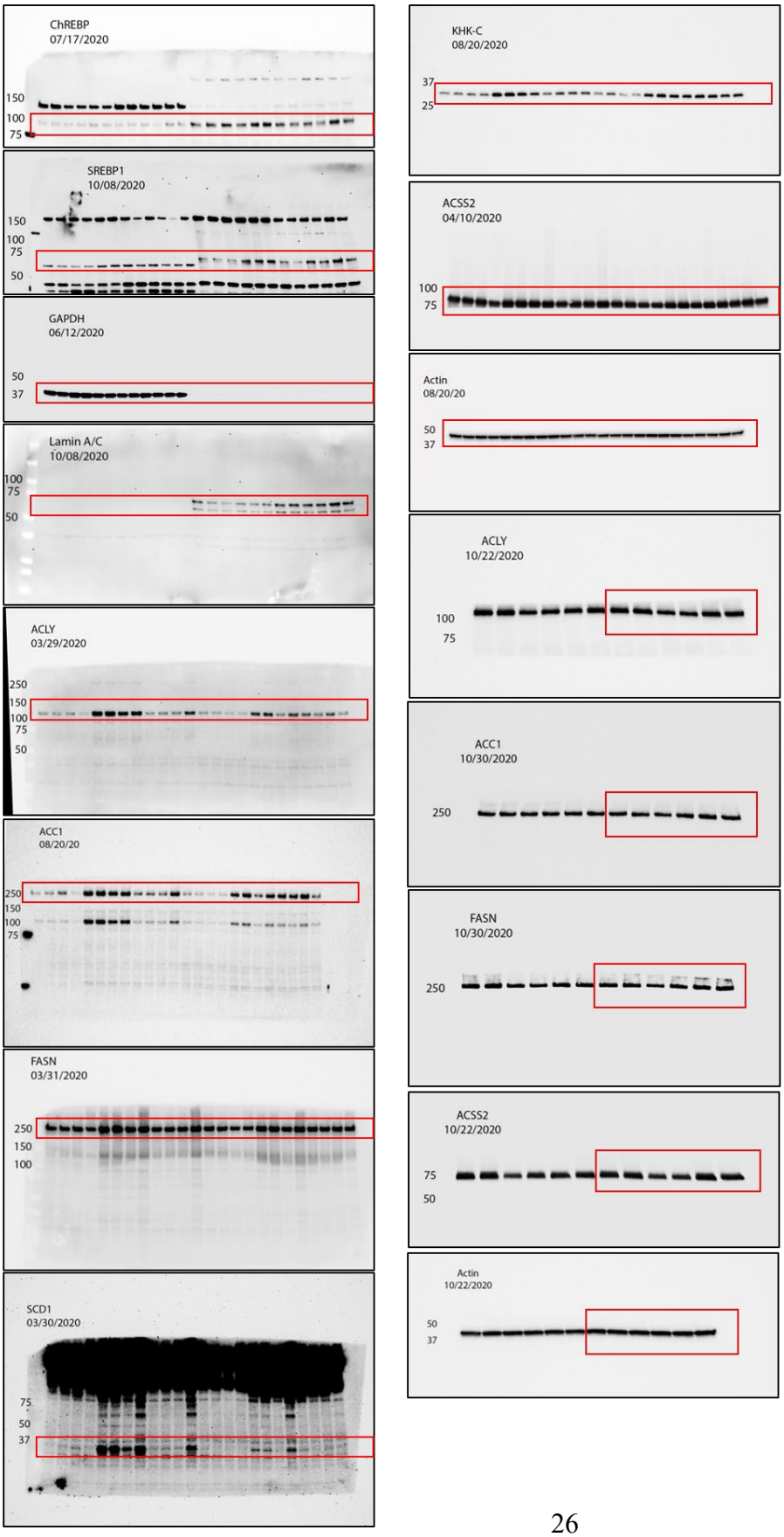

Supplemental Figure 12 – Blots from Figure 3

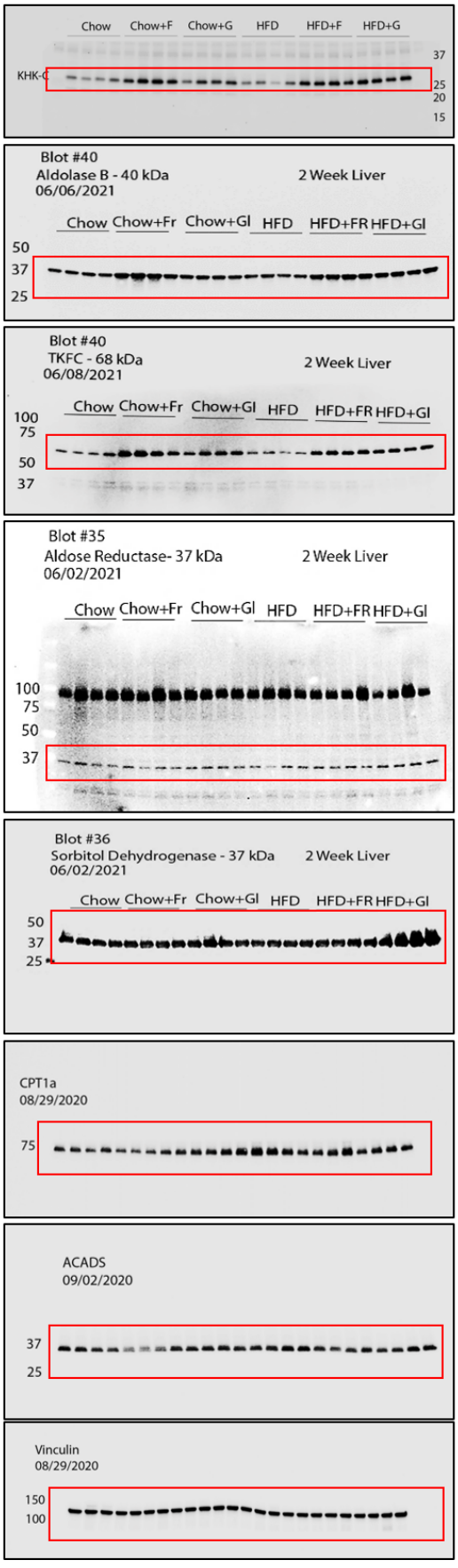

Supplemental Figure 13 – Blots from Figure 4

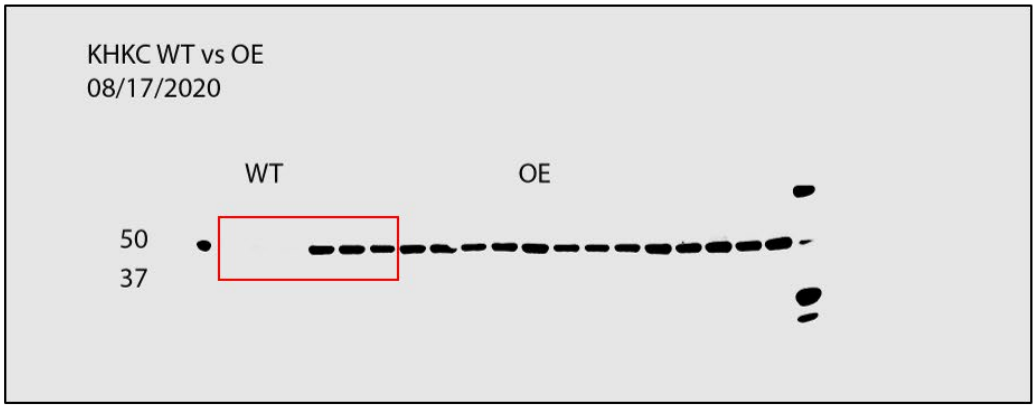

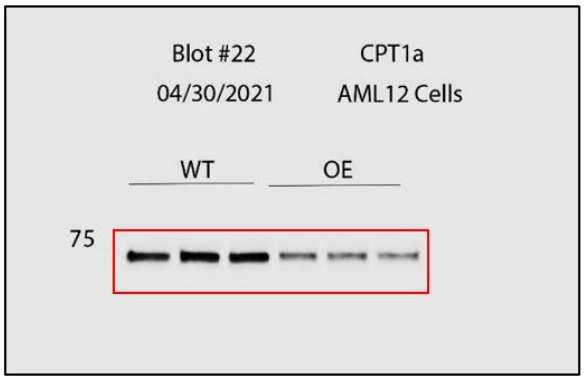

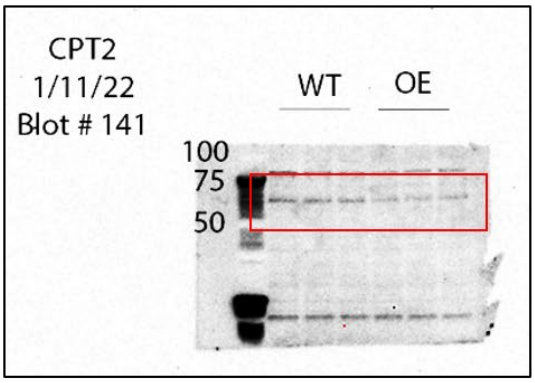

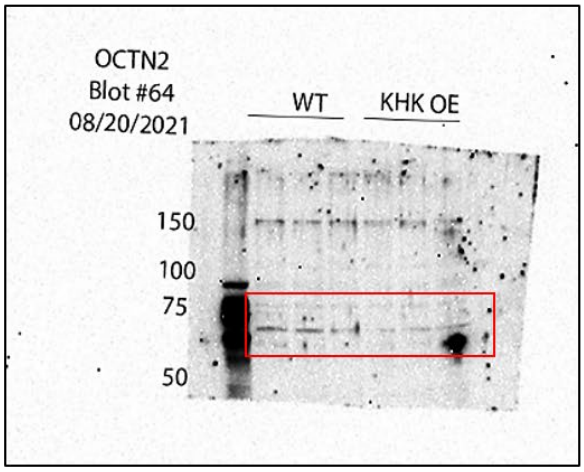

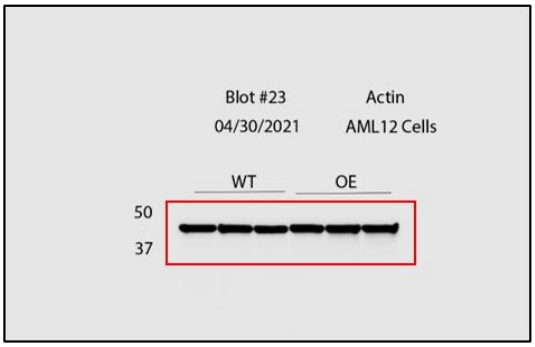

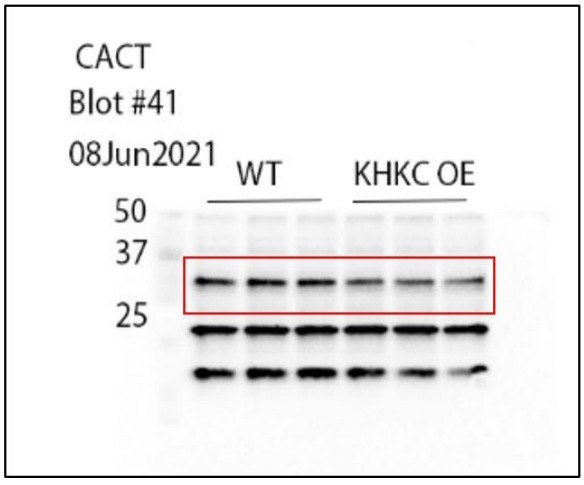

Supplemental Figure 14 – Blots from Figure 5

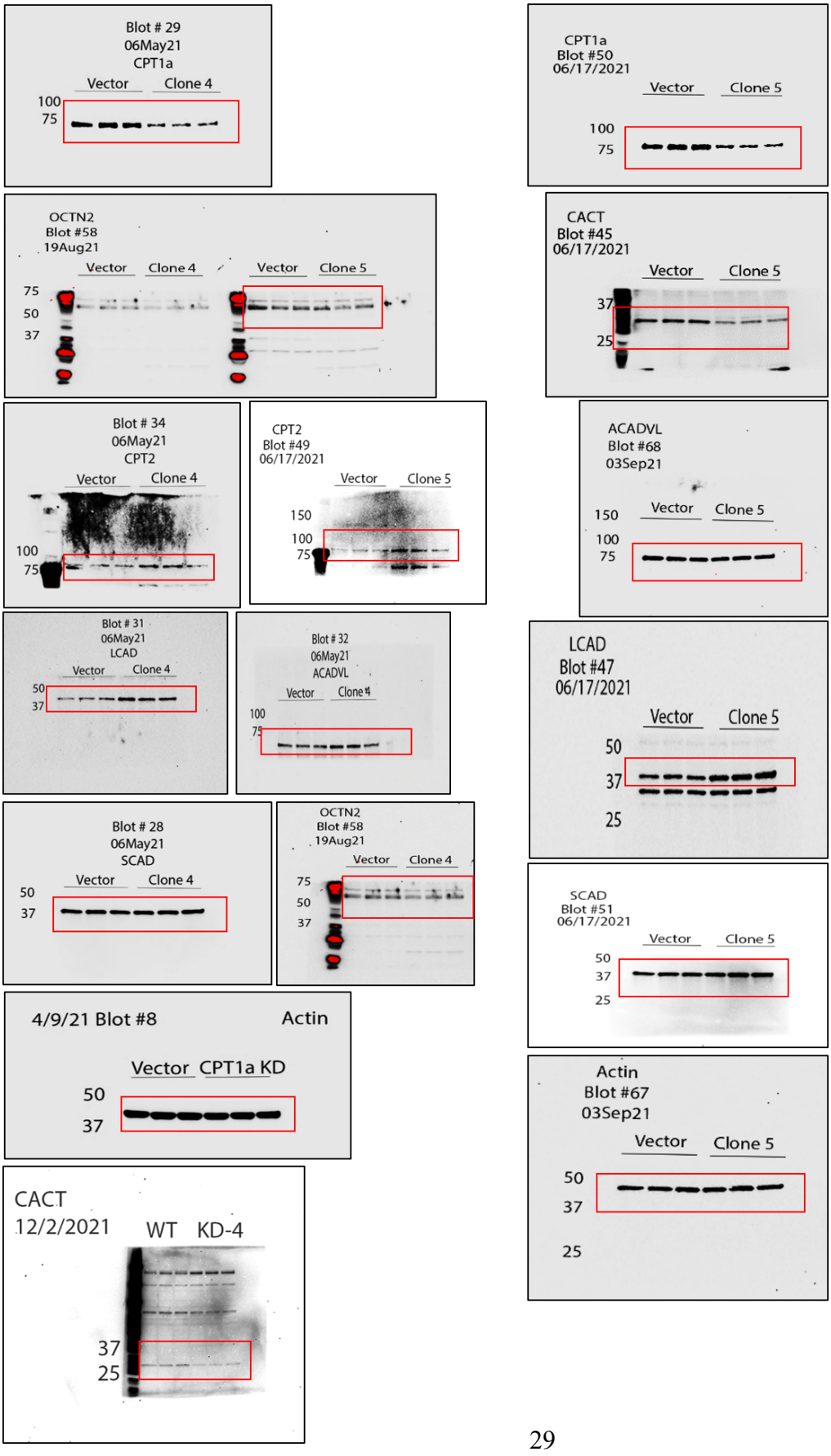

Supplemental Figure 15 – Blots from Figure 5 Continued

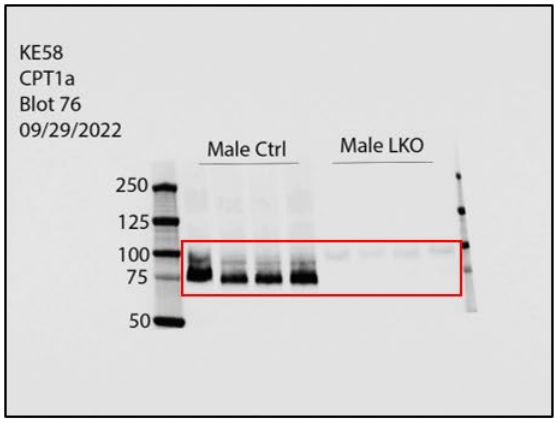

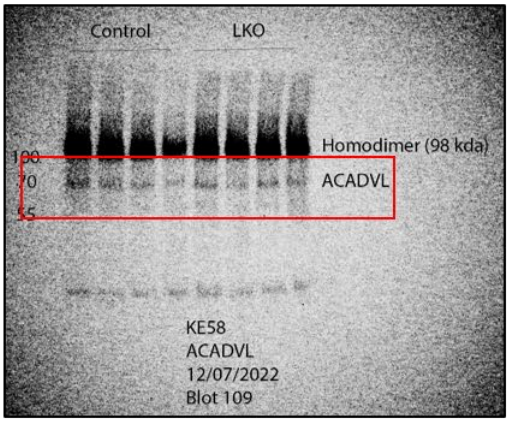

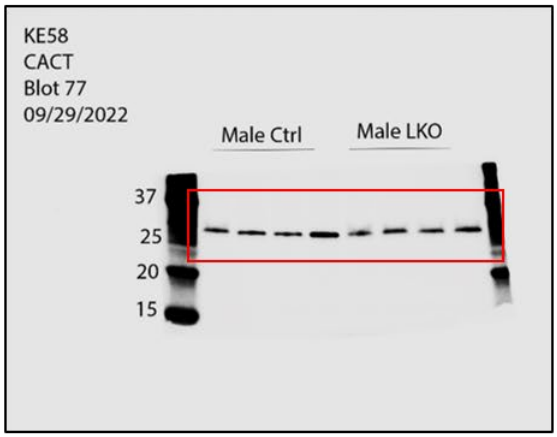

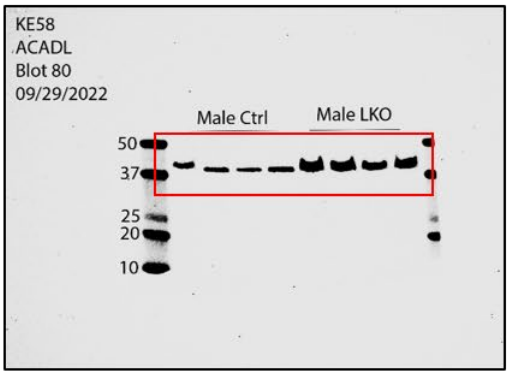

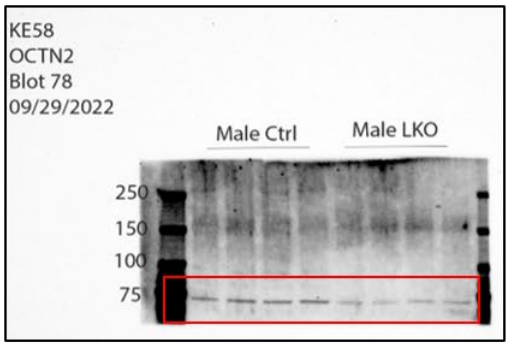

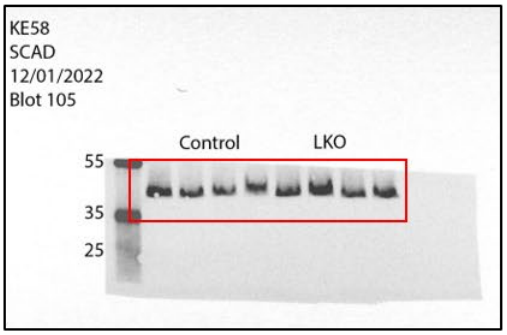

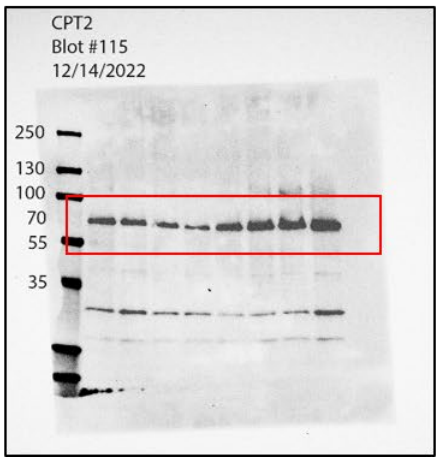

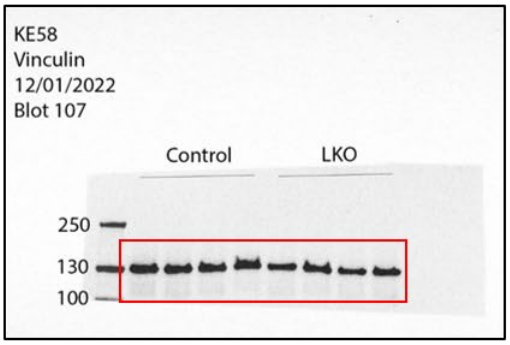

Supplemental Figure 16 – Blots from Figure 6

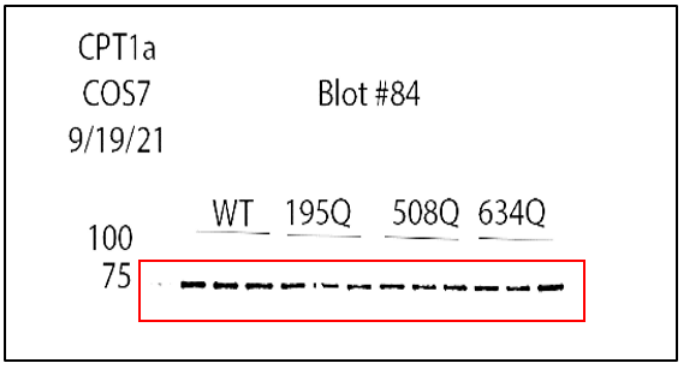

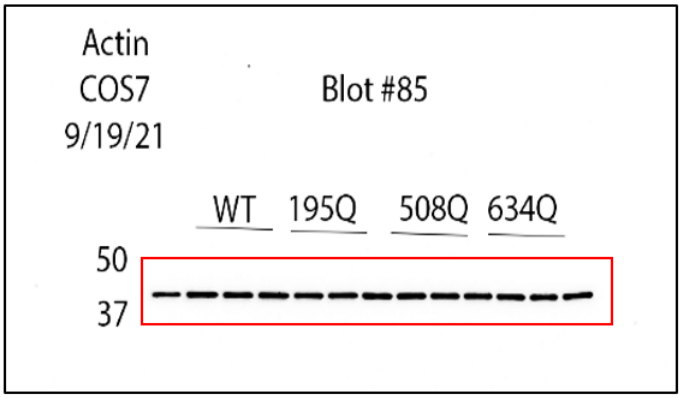

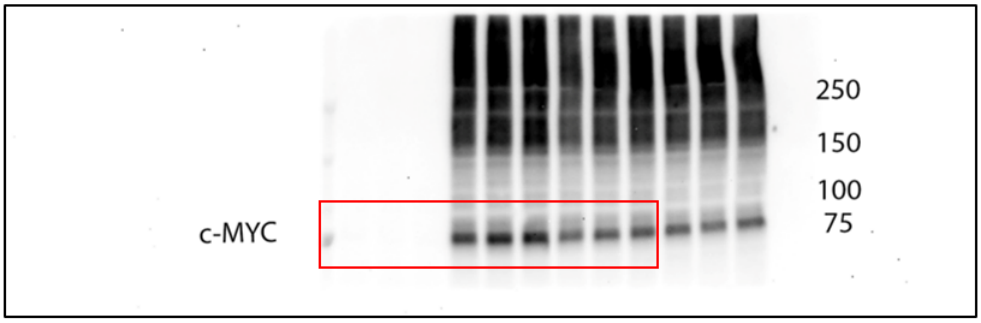

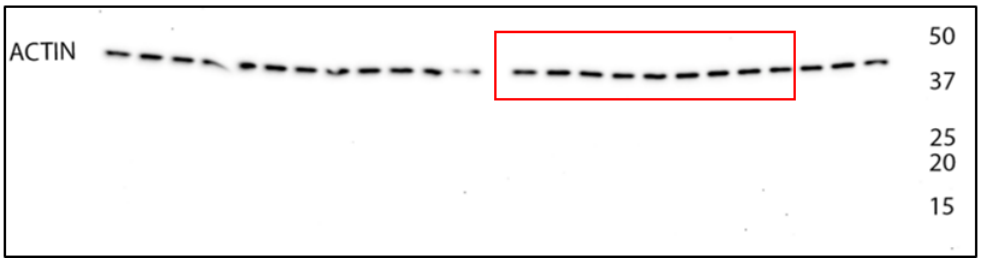

Supplemental Figure 17 – Blots from Figure 7

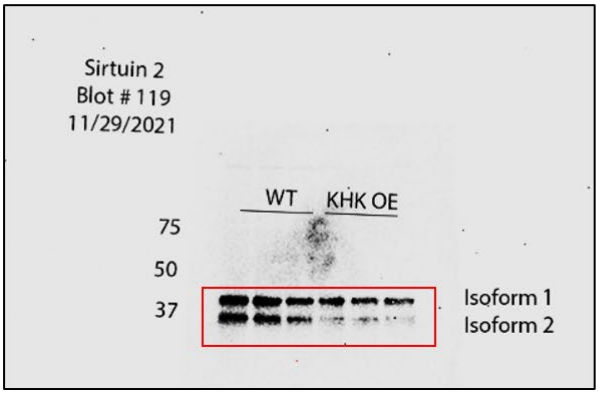

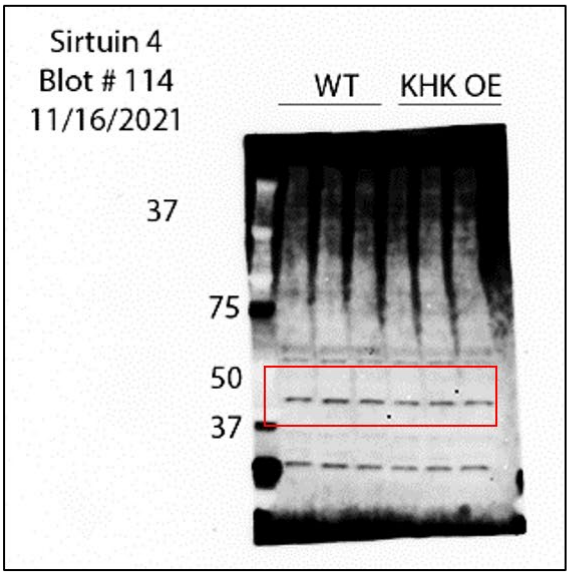

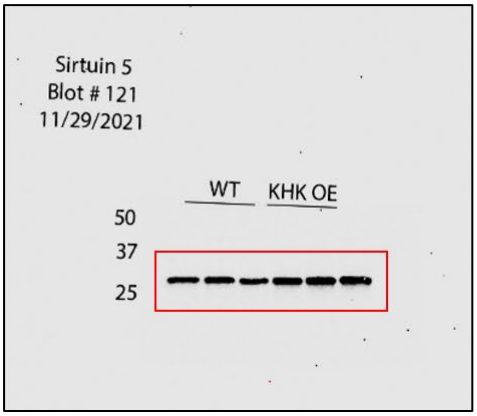

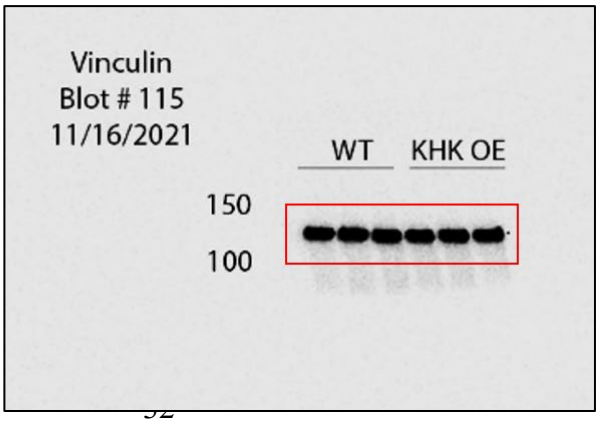

Supplemental Figure 18 – Blots from Supplemental Figure 1

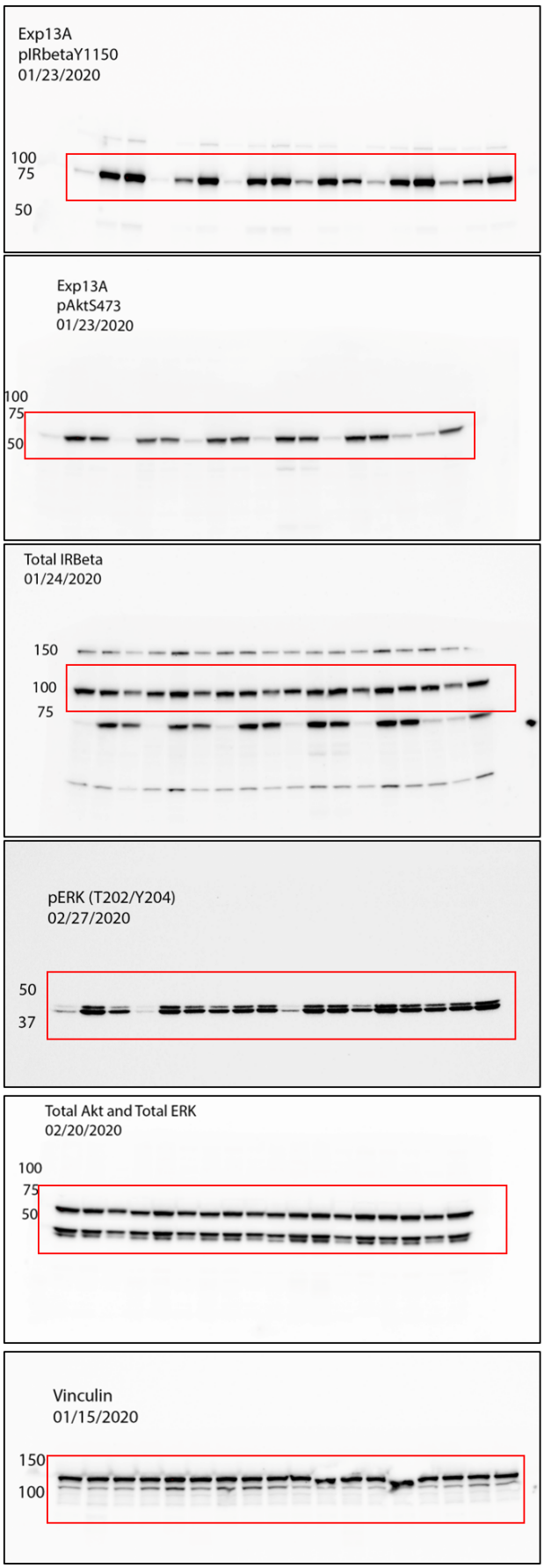

Supplemental Figure 19 – Blots from Supplemental Figure 2

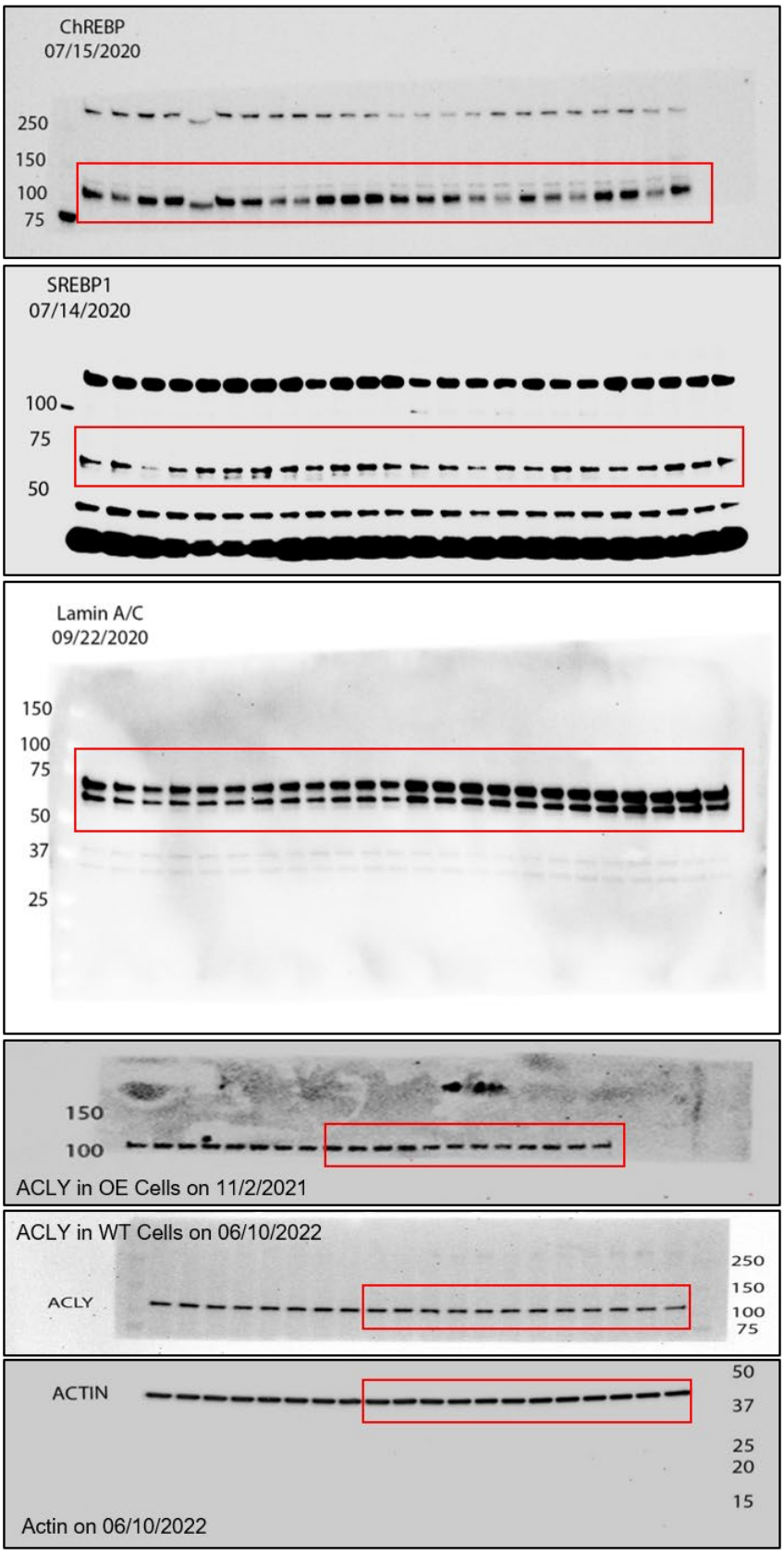

Supplemental Figure 20 – Blots from Supplemental Figure 4

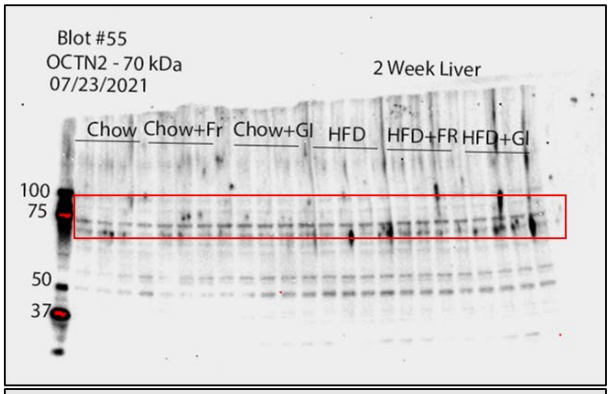

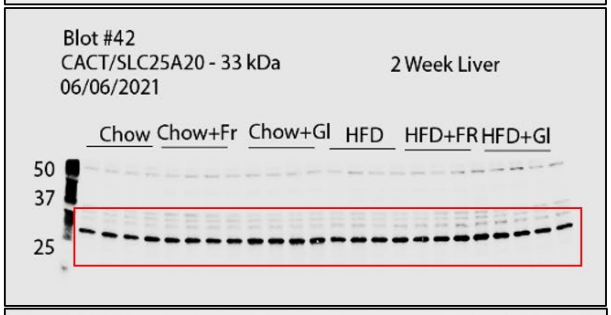

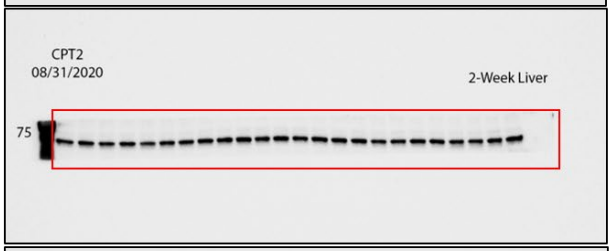

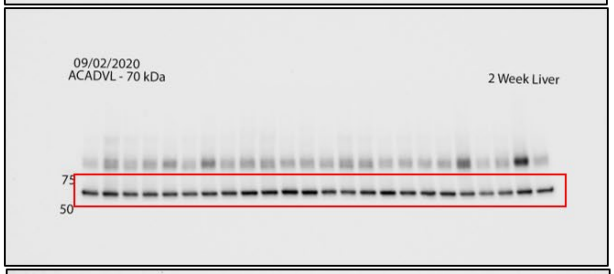

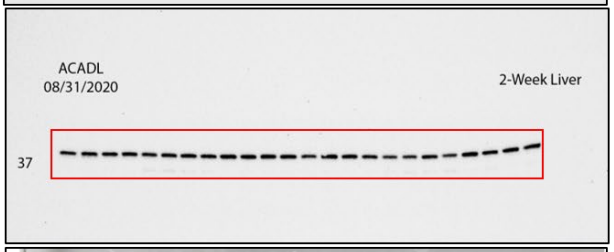

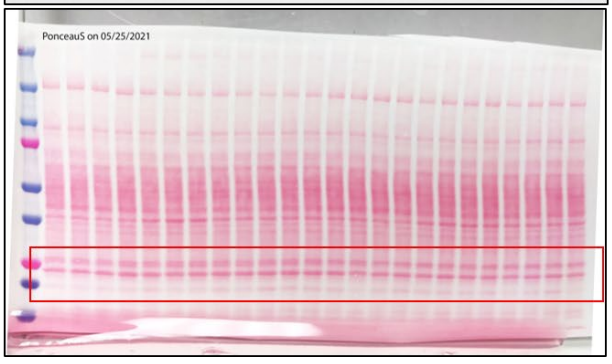

Supplemental Figure 21 – Blots from Supplemental Figure 5

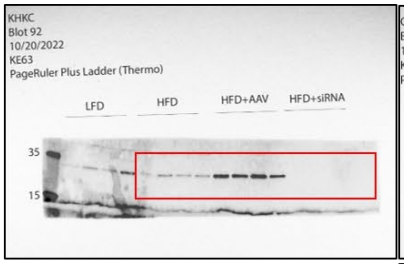

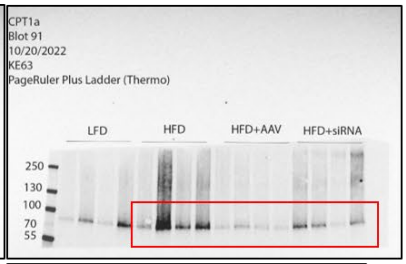

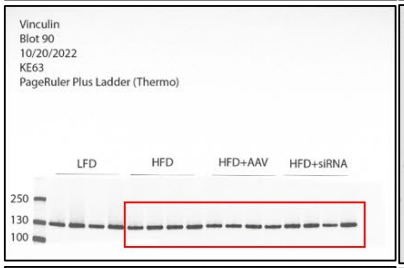

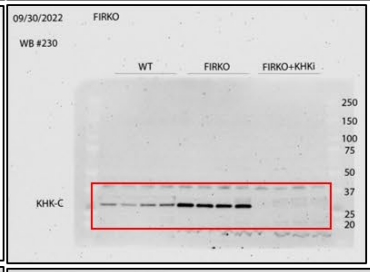

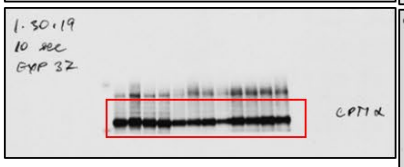

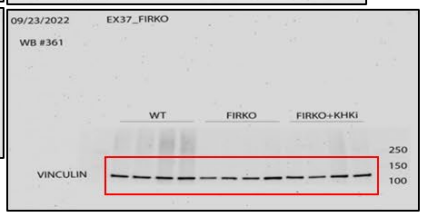

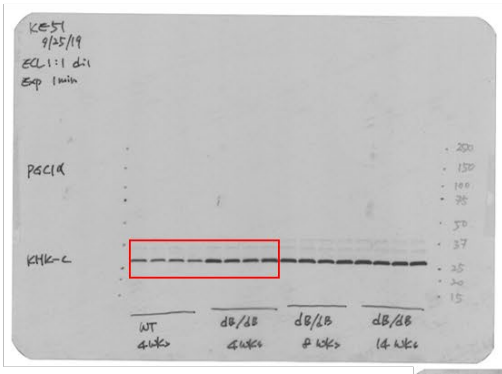

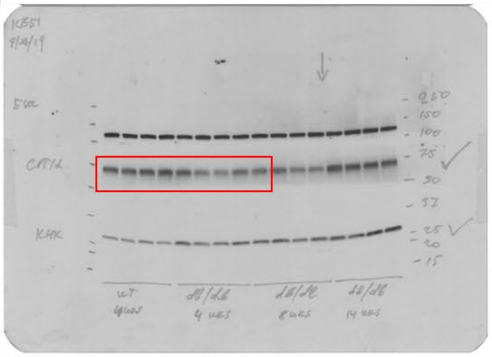

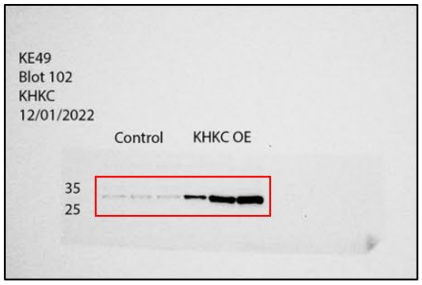

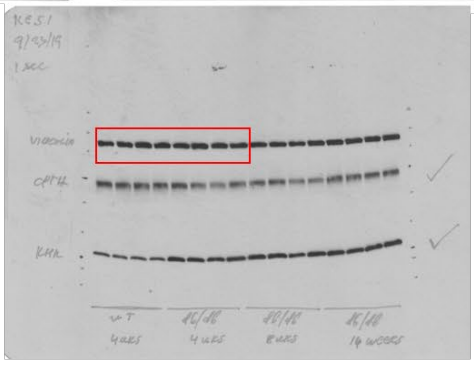

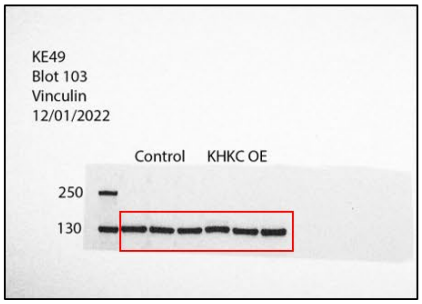

Supplemental Figure 22 – Blots from Supplemental Figure 6

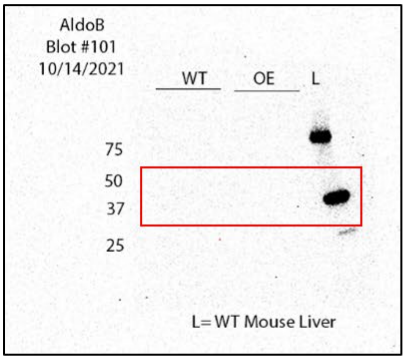

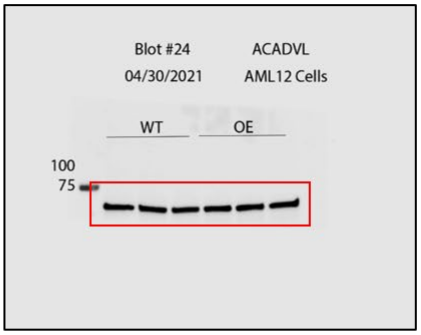

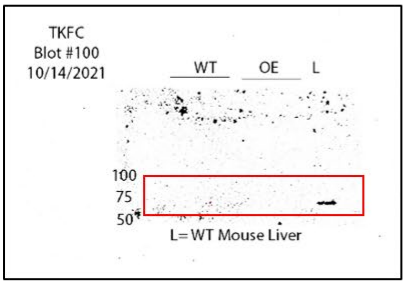

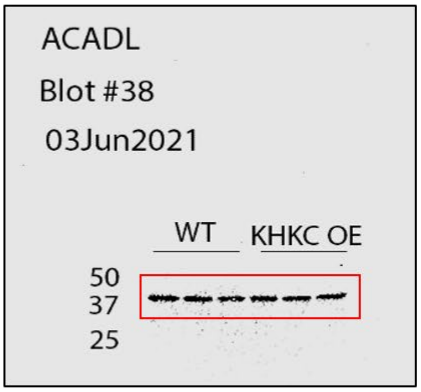

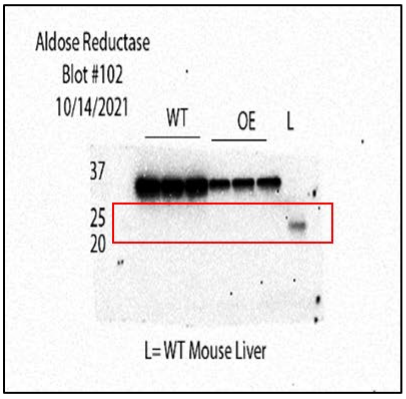

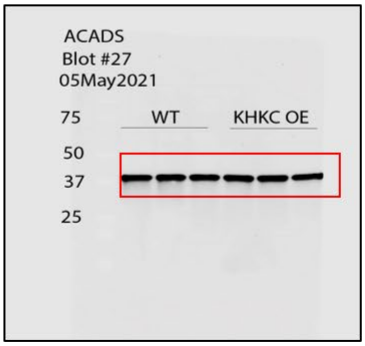

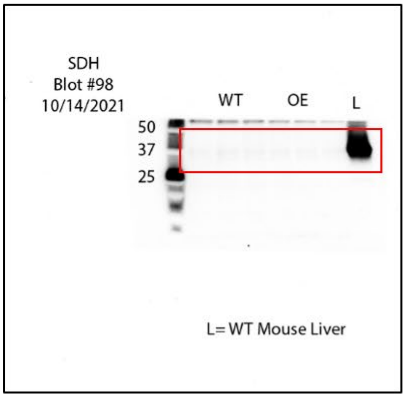

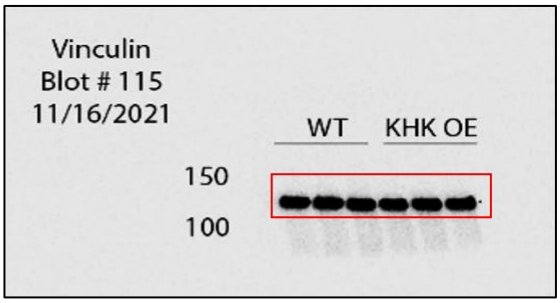

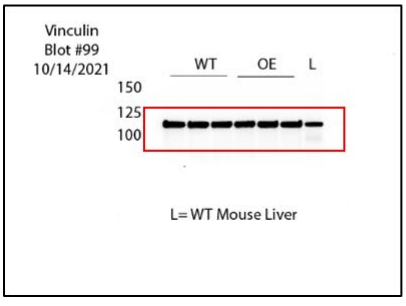

Supplemental Figure 23 – Blots from Supplemental Figure 8

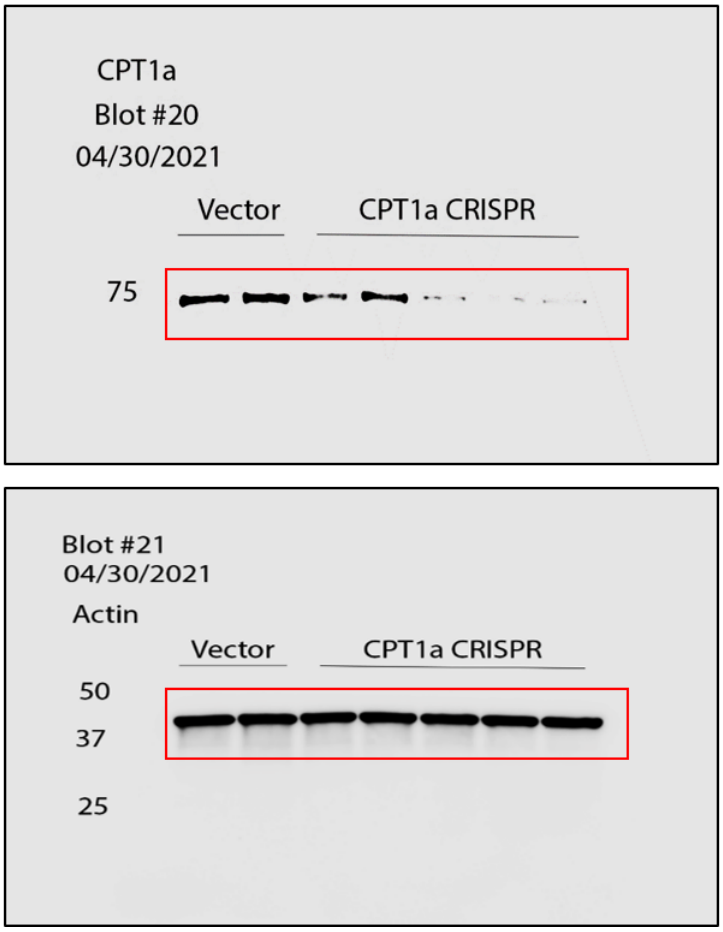

Supplemental Figure 24 – Blots from Supplemental Figure 10

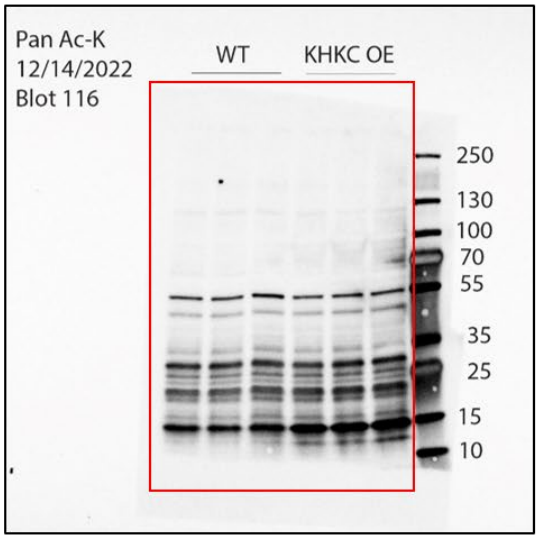

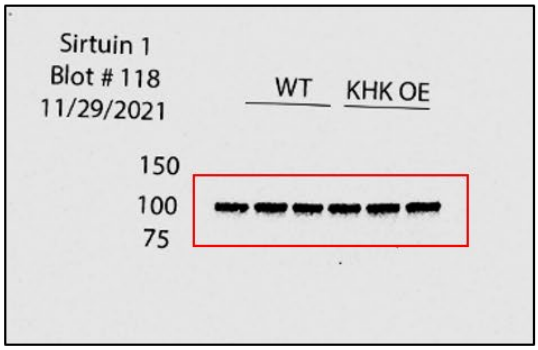

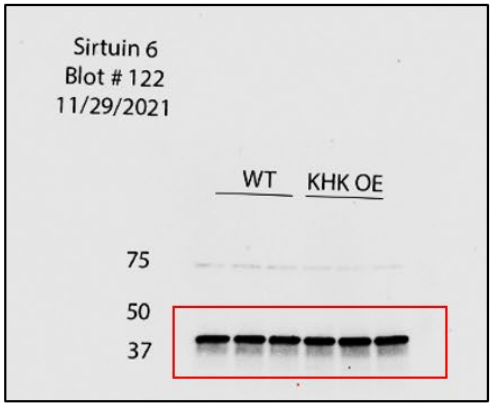

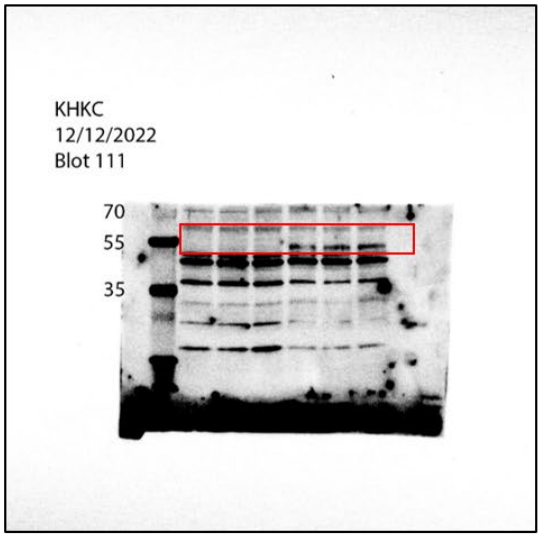

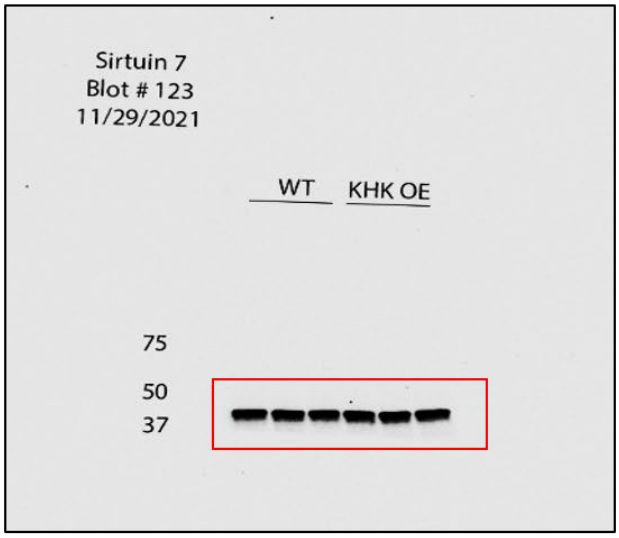

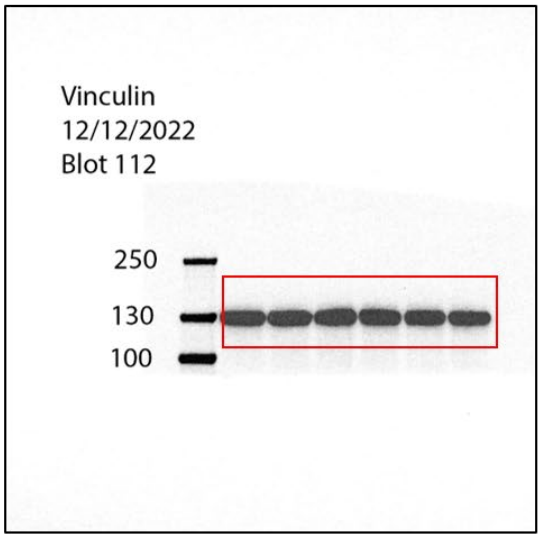

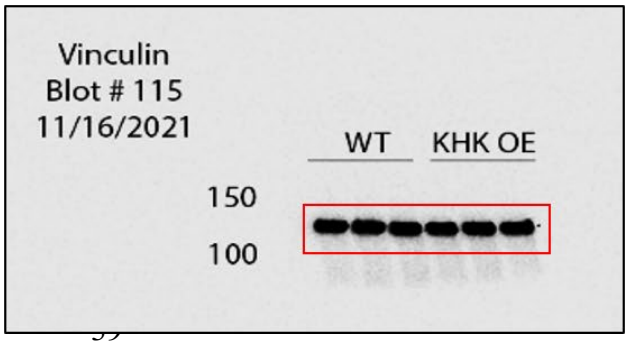

Supplemental Figure 25 – Blots from Supplemental Figure 10 Continued

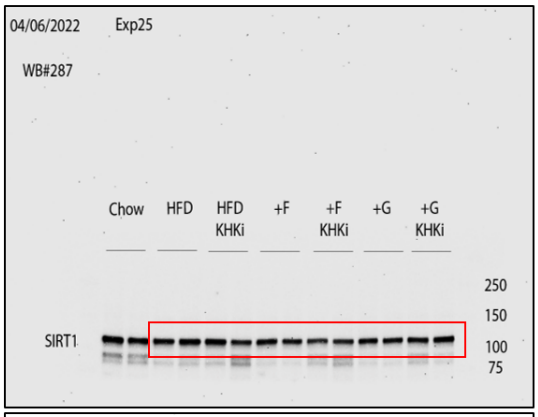

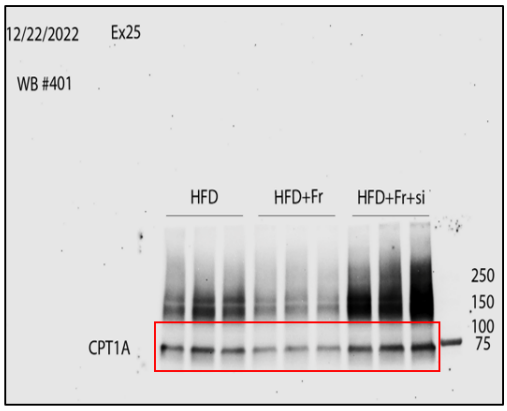

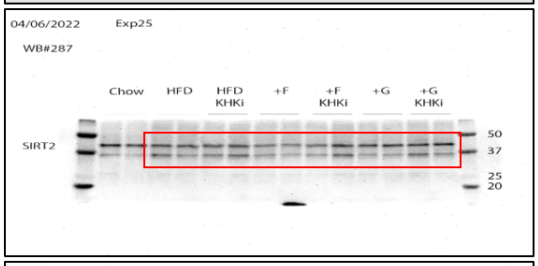

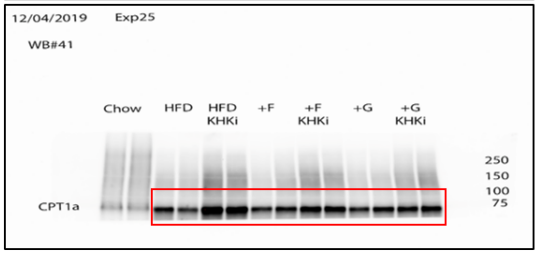

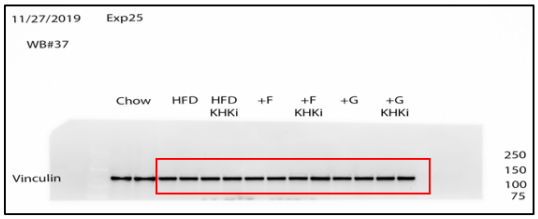

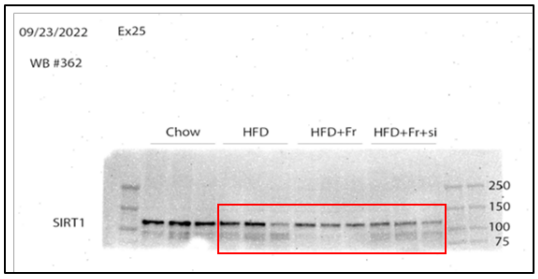

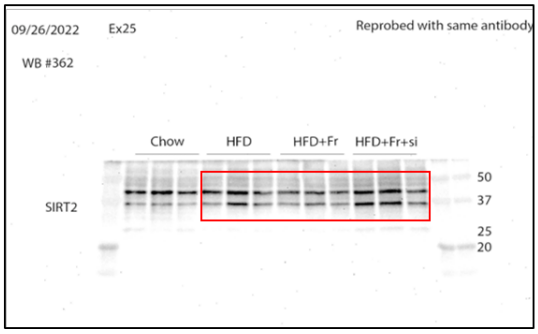

Supplementary tables

Table S1. Acetylome analysis in WT and KHK-C OE AML-12 cells

See attached

Table S2. Proteome analysis in WT and KHK-C OE AML-12 cells

See attached

Table S3. Mouse primers used for real-time quantitative PCR.

Gene	Sequence (5' – 3')	Forward/Reverse
Acly	CAGCCAAGGCAATTTCAGAGC	Forward
	CTCGACGTTTGATTAACTGGTCT	Reverse
Acc1	ACAGTGGAGCTAGAATTGGAC	Forward
	ACTTCCCGACCAAGGACTTTG	Reverse
Fasn	GGAGGTGGTGATAGCCGGTAT	Forward
	TGGGTAATCCATAGAGCCCAG	Reverse
Scd1	CAGCCGAGCCTTGTAAGTTC	Forward
	GCTCTACACCTGCCTCTTCG	Reverse
Chrebp-b	TCTGCAGATCGCGTGGAG	Forward
	CTTGTCCCGGCATAGCAAC	Reverse
Acsl1	TGCCAGAGCTGATTGACATTC	Forward
	GGCATACCAGAAGGTGGTGAG	Reverse
Acss2	AGGTGACCAAGTTCTACACGGC	Forward
	GTTGATGGGTTCACCTACTGTGC	Reverse
Khk-c	AACTCCTGCACTGTCCTTTCCTT	Forward
	CCACCAGGAAGTCGGCAA	Reverse
Aldob	GCTGGGCAATTTCAGAGAGC	Forward
	GAGGACTCTTCCCCTTTGCT	Reverse
Tkfc	CCTTGCTGGGTTAGTAGCCTC	Forward
	CTTTCCCGATAAAACCGGCAT	Reverse
Ar	AGGCCGTGAAAGTTGCTATTG	Forward
	ATGCTCTTGTCATGGAACGTG	Reverse
Sdh	GCTAAGGGCGAGAACCTGTC	Forward
	CATGCTCCCAGTAGTGAACATC	Reverse
Octn2	AAGACCTGCAGGAAGCTGAA	Forward
	TCCTTGTTTTTCGTGGGTGT	Reverse
Cact	GGTGGCTGTCCAGACAAACT	Forward
	TCCGTTTAAGAACCTCCTGG	Reverse
Crat	CTCCTGGGCTGGAGTAGATG	Forward
	TTACAGAAGGGACTGGAGCG	Reverse
Acadvl	CTGATGAGCTCCCAGGGTAA	Forward
	TTGGGCCTCTCTAATACCCA	Reverse
Acadl	TCTTGCGATCAGCTCTTTCA	Forward
	GGTACATGTGGGAGTACCCG	Reverse
Acadm	GCGAGCAGAAATGAAACTCC	Forward
	AGCTCTAGACGAAGCCACGA	Reverse
Acads	TGGCGACGGTTACACACTG	Forward
	GTAGGCCAGGTAATCCAAGCC	Reverse

Cpt1a	AGTGGCCTCACAGACTCCAG	Forward
	GCCCATGTTGTACAGCTTCC	Reverse
Khk-a	TTGCCGATTTTGTCCTGGAT	Forward
	CCTCGGTCTGAAGGACCACAT	Reverse
Phgdh	ATGGCCTTCGCAAATCTGC	Forward
	AGTTCAGCTATCAGCTCCTCC	Reverse
Psat1	CAGTGGAGCGCCAGAATAGAA	Forward
	CCTGTGCCCCTTCAAGGAG	Reverse
Psph	AGGAAGCTCTTCTGTTCAGCG	Forward
	GAGCCTCTGGACTTGATCCC	Reverse
18S	GTAACCCGTTGAACCCCATT	Forward
	CCATCCAATCGGTAGTAGCG	Reverse
Tbp	TGACTGCAGCAAATCGCTTGG	Forward
	ACCCTTCACCAATGACTCCTATG	Reverse

Table S4. CRISPR/Cas9 guides used for knockdown of *Cpt1a*.

Gene	**Sequence (5' – 3')**	**Forward/Reverse**
Cpt1a Guide 1	CACCGTAACAGCAACTACTACGCCA	Forward
	AAACTGGCGTAGTAGTTGCTGTTAC	Reverse
Cpt1a Guide 2	CACCGTGATCGGCCCTCGGCCCCGC	Forward
	AAACGCGGGGCCGAGGGCCGATCAC	Reverse
U6 (sequencing)	ACTATCATATGCTTACCGTAAC	Forward

Table S5. Isolation scheme for proteome and acetylome analysis

Table S6: Isolation scheme of the DIA method.

Window	Start m/z	Stop m/z	Center m/z	z	I
1	350	383	366.5	3	
2	382	408	395	3	
3	407	429	418	3	
4	428	448	438	3	
5	447	467	457	3	
6	466	484	475	3	
7	483	503	493	3	
8	502	521	511.5	3	
9	520	539	529.5	3	
10	538	557	547.5	3	
11	556	575	565.5	3	
12	574	594	584	3	
13	593	614	603.5	3	
14	613	634	623.5	3	
15	633	656	644.5	3	
16	655	678	666.5	3	
17	677	701	689	3	
18	700	726	713	3	

19	725	756	740.5	3
20	755	787	771	3
21	786	823	804.5	3
22	822	862	842	3
23	861	914	887.5	3
24	913	979	946	3
25	978	1077	1027.5	3
26	1076	1650	1363	3

Supplementary references

[1] Helsley RN, Miyata T, Kadam A, Varadharajan V, Sangwan N, Huang EC, et al. Gut microbial trimethylamine is elevated in alcohol-associated hepatitis and contributes to ethanol-induced liver injury in mice. Elife 2022;11.

[2] Helsley RN, Varadharajan V, Brown AL, Gromovsky AD, Schugar RC, Ramachandiran I, et al. Obesity-linked suppression of membrane-bound O-acyltransferase 7 (MBOAT7) drives non-alcoholic fatty liver disease. Elife 2019;8.

[3] Softic S, Meyer JG, Wang GX, Gupta MK, Batista TM, Lauritzen H, et al. Dietary Sugars Alter Hepatic Fatty Acid Oxidation via Transcriptional and Post-translational Modifications of Mitochondrial Proteins. Cell Metab 2019;30:735-753 e734.

[4] Park SH, Helsley RN, Noetzli L, Tu HC, Wallenius K, O'Mahony G, et al. A luminescence-based protocol for assessing fructose metabolism via quantification of ketohexokinase enzymatic activity in mouse or human hepatocytes. STAR Protoc 2021;2:100731.

[5] Ran FA, Hsu PD, Wright J, Agarwala V, Scott DA, Zhang F. Genome engineering using the CRISPR-Cas9 system. Nat Protoc 2013;8:2281-2308.

[6] Softic S, Gupta MK, Wang GX, Fujisaka S, O'Neill BT, Rao TN, et al. Divergent effects of glucose and fructose on hepatic lipogenesis and insulin signaling. J Clin Invest 2017;127:4059-4074.

[7] Lei XH, Bochner BR. Optimization of cell permeabilization in electron flow based mitochondrial function assays. Free Radic Biol Med 2021;177:48-57.

[8] Escher C, Reiter L, MacLean B, Ossola R, Herzog F, Chilton J, et al. Using iRT, a normalized retention time for more targeted measurement of peptides. Proteomics 2012;12:1111-1121.

[9] Collins BC, Hunter CL, Liu Y, Schilling B, Rosenberger G, Bader SL, et al. Multi-laboratory assessment of reproducibility, qualitative and quantitative performance of SWATH-mass spectrometry. Nat Commun 2017;8:291.

[10] Gillet LC, Navarro P, Tate S, Rost H, Selevsek N, Reiter L, et al. Targeted data extraction of the MS/MS spectra generated by data-independent acquisition: a new concept for consistent and accurate proteome analysis. Mol Cell Proteomics 2012;11:O111 016717.

[11] Bruderer R, Bernhardt OM, Gandhi T, Xuan Y, Sondermann J, Schmidt M, et al. Optimization of Experimental Parameters in Data-Independent Mass Spectrometry Significantly Increases Depth and Reproducibility of Results. Mol Cell Proteomics 2017;16:2296-2309.

[12] Burger T. Gentle Introduction to the Statistical Foundations of False Discovery Rate in Quantitative Proteomics. J Proteome Res 2018;17:12-22.

[13] Rohart F, Gautier B, Singh A, Le Cao KA. mixOmics: An R package for 'omics feature selection and multiple data integration. PLoS Comput Biol 2017;13:e1005752.

[14] Kamburov A, Pentchev K, Galicka H, Wierling C, Lehrach H, Herwig R. ConsensusPathDB: toward a more complete picture of cell biology. Nucleic Acids Res 2011;39:D712-717.

[15] Kamburov A, Wierling C, Lehrach H, Herwig R. ConsensusPathDB--a database for integrating human functional interaction networks. Nucleic Acids Res 2009;37:D623-628.

[16] Wickham H. ggplot2 : Elegant Graphics for Data Analysis. Use R!,, 2nd ed. Cham: Springer International Publishing : Imprint: Springer,; 2016. p. 1 online resource (XVI, 260 pages 232 illustrations, 140 illustrations in color.